Responses to editor and reviewer comments on "Model estimates of climate controls on pan-Arctic wetland methane emissions" by X. Chen et al.

Editor

Referee 1 asks for a more detailed validation of the model, noting a lack of uncertainty estimates around the simulations, and minimal comparison to independent data or models. I agree that this is a significant lack in the current ms, so please address this issue in detail. To have confidence in the simulations we need a thorough assessment of model error ('error' is a word I cannot see in the text!). I would be interested to know how uncertainty in the W&H parameters (table 1) is propagated into the simulations. How is uncertainty in ebullition (related to sedge cover, oxidation fraction) dealt with, as these parameters seem highly uncertain? What is the error associated with the assignments of north and south parameters across the high latitudes, particularly outside Siberia where they were developed?

Thank you for your comments. Regarding validation of the model: we have indeed compared our framework to in situ observations across West Siberia, in Bohn et al. (2013), although this did not evaluate temporal behavior. We compared our model's temporal variability against independent models and inversions over the West Siberian Lowland over the period 1992-2010, in Bohn et al. (2015), and found that our model compared favorably to the Bousquet et al. (2011) inversion. As an aside, Bohn et al. (2015) also showed that the inversions themselves displayed suspicious behaviors, including setting all net wetland CH_4 emissions < 0 over all of boreal Asia in some years; similarly, the Bloom et al. (2010) gridded CH_4 product showed essentially no interannual variability; thus we are not convinced that inversions or other gridded products are any better than process-based models in this regard. We have added a brief discussion to this effect in the discussion section.

We agree that assessment of the robustness of our findings under parameter uncertainty is warranted. We have addressed this issue in the revised paper as follows:

1. To address uncertainty in the boundary between the regions using the north and south parameter sets, we performed two additional simulations: "all-south" and "all-north", in which the south and north parameter sets (respectively) were applied over the entire domain.
2. We have replaced the single sensitivity-based simulation and projection with an ensemble of 20 simulations, with sensitivities derived from a similar ensemble of 20 historical process-based projections, 18 of which have parameters randomly sampled from their posterior distributions as reported in Bohn et al. (2013), and two of which consist of the all-south and all-north simulations. We have added an

additional variable to the set of parameters whose uncertainty we explored (and which was also randomly sampled in the ensemble): Tveg, which controls the strength of plant-aided transport. We have expanded Table 1 to show the posterior distributions of parameter values from Bohn et al. (2013) (and Tveg), instead of only the median (note also that the parameter values originally listed in Table 1 were not correct).

3. Uncertainty in root zone oxidation, controlled by the parameter Pox (which sets the fraction of methane that is oxidized in the root zone), was not added to the analysis, because it is redundant with Tveg in the W&H model. Its only use in the model is to reduce the amount of CH_4 that participates in plant-aided transport:

$$Qplant = Tveg*(1-Pox)*(other\ factors\ including\ root\ density)$$

Because Tveg is also not used anywhere else in the model, any given change in Pox can be compensated for by a corresponding change in Tveg. Thus, we opted to hold Pox constant at a value of 0.5 (as in the original W&H model) and only vary Tveg. We have added a note to this effect in the methods section.

4. We have incorporated the results from this parameter uncertainty ensemble into our figures as follows: Figure 7: in addition to the existing map (for the median parameter values), we show another map illustrating the range in P- and T-correlations across the uncertainty ensemble at each point. Figure 9: in addition to the existing matrices of sensitivities (for the median parameter values) we show maps of the range of sensitivities across the ensemble. Figure 10: we use the results from the ensemble to create envelopes at confidence intervals about the existing historical and future emissions time series. Figures 11 and 12: we have reduced the number of time slices we consider to only the final end-of-century window, and have added maps showing the ranges of future emissions (Fig 11) and T-/P-correlations (Fig 12) across the ensemble.

Referee 2 asks for more details on how precipitation and temperature control CH4 response through wetland extent dynamics. Please provide further details to resolve this issue, as it represents a novelty of your approach.

Here we paraphrase our response to referee 2: We assume by "wetland area" the reviewer is referring to "inundated area". We have added an analysis of inundation area over the historical period: 1) We have added a map (figure 13) showing the changes in inundation area and water table level from each wetland grid cell between the periods 1960-2006 and 2081-2100; 2) We have included a paragraph in the manuscript that talks about this change, as well as its possible relations to changes in the methane emitted from the wetland. We have also calculated a spatial correlation coefficient between changes in

inundation fractions, and changes in methane emitted, to check whether they are spatially correlated.

Anonymous Referee #1

The authors use a land-surface process-based model to identify the dominant climate drivers of northern high-latitude wetland methane (CH4) emissions, and to estimate present-day and future CH4 emissions from Arctic wetlands. The authors quantify the model CH4 emission sensitivity to precipitation, temperature, radiation and CO2. The process-based model and the sensitivities are both used to derive 21st century methane emissions based on CMIP5 climate driver projections. The study results show that CH4 emissions will be 42% higher in the 21st century, relative to 1997-2006. The manuscript is clearly written: the methodology is well documented, and the results are clearly presented.

We thank the reviewer for the detailed comments that helped improve our manuscript, especially regarding uncertainties. Our responses to all the comments are listed below.

A major shortcoming of the work presented in this manuscript is that the wetland CH4 emission climate sensitivity and 21st century predictions are wholly contingent on the model used in this study. However, the authors do not attempt quantify or explore the structural and/or parametric model uncertainty. Given that model parameters are a major source of uncertainty in future flux projections in the carbon cycle (e.g. Booth et al., 2012), I strongly recommend that the authors quantify or characterize the sensitivity of their results to model parameters controlling methane emissions.

To quantify the uncertainties in our results, we performed several new runs that take the uncertainties of methane model parameters into consideration, following a similar approach to the experiments in Bohn et al. (2013). The details of the uncertainty analyses are now included in a new section, section 2.7. We have updated figure 9 to include a new set of panels that show ranges in climate sensitivity values at 95% confidence level. We also performed uncertainty analyses on our future projections, and have updated our figure 10 to include the 95% confidence bounds. While the parameter uncertainty added uncertainty to our estimates of total emissions, it did not change the nature of T- or P-limitation in any substantial way. However, we recognize that our results are still contingent on our model formulation. We address this in the Discussion section.

It is also unclear whether the model can adequately simulate the inter-annual variability of wetland CH4 emissions: although the authors have compared the mean annual model wetland CH4 emissions against a range estimates, the temporal variability of modeled wetland CH4 fluxes has not been compared against other bottom-up/topdown estimates or in-situ measurements. Given that the seasonal and inter-annual variations of the model's wetland CH4 emissions - and their response to climatic variability - are a fundamental component of the work presented in this manuscript, the authors should compare the temporal variability of CH4 emissions against at least one (if not all) of the following: in-situ measurements, atmospheric inversion CH4 estimates, other model results (e.g. Melton et al., 2013).

Interannual variability is an important metric of simulation quality. Unfortunately, there are very few in situ observations in the domain that have sufficiently long record lengths (>= 10 years) that could help constrain model interannual variability. In terms of comparisons with inversions and other large-scale models, Bohn et al. (2015) compared the time series of annual emissions over the Western Siberian Lowland (part of the pan-Arctic area) from 21 models, including our model formulation (UW-VIC), to those of three atmospheric inversions (two from Bousquet et al., 2011 and one from Bloom et al., 2010) over the period 1993-2010, and found that, while none of the models had high correlations with the inversions, UW-VIC was among the few models that shared similar behavior with the inversions (namely, low correlations with either summer inundated area or summer air temperature). Those models with higher correlations with inundation or temperature tended to do so as a result of flaws in their model formulations. Further, the inversions themselves showed some suspicious behaviors, with one of the Bousquet inversions reaching net negative emissions over all of boreal Asia in some years, and the Bloom inversion showing almost no interannual variability. Therefore, we argue that our model has already been sufficiently evaluated in terms of interannual variability. We have added a short discussion of this point to the Discussion section.

Finally, the authors categorize the sensitivity of wetland CH4 emissions with respect to June-August precipitation (P) & temperature (T), however both observations and models suggest substantial wetland CH4 emissions in September/October (Chang et al., 2014, Mastepanov et al., 2008, Melton et al., 2013), and hence September/October P and T undoubtedly play an important role. The authors should either extend this period to include September, or should explicitly state why September/October T and P were omitted.

Our sensitivity estimates do include the September/October P and T influence, because we calculated the sensitivities of annual CH_4 to annual P, T and CO_2 (the control runs affected climate year-round). What may have confused the reviewer is that we averaged these sensitivities over all grid cells that had similar JJA P and JJA T. I.e., we computed the average sensitivity to annual climate as a function of JJA climate. The reason for this is that CH_4 emissions occur primarily during the growing season, and are therefore much more highly correlated with JJA T and P than with annual T and P. We have updated section 2.4 in our text to make this clearer. Also, we highlight this again in the notation of figure 9.

Specific comments

Throughout the manuscript: The term "Arctic" is misleading, given that the study region includes all wetland CH4 emissions at latitudes >45N. Please consider revising.

It is true that the domain contains land that is outside of the Arctic Circle. However, several studies (e.g., Su et al., 2006; Slater et al., 2007; Zhu et al., 2013) have used the term "pan-Arctic" to refer to the Arctic terrestrial drainage basin, i.e., all land that drains into the Arctic Ocean. Our domain is similar to that domain, with the exception that it also contains Tibet. We have added an appropriate clarification to Section 2.1.

P5942 L15-L18: "Over the entire period 1948–2006, our reconstructed CH4 emissions increased by 20%, over 90% of which can be attributed to climate change. An increasing trend in summer air temperature explained the majority of the climate-related variance". Climate change is a broad term. Please rephrase and/or be more specific.

This is now rewritten as "Over the entire period 1948–2006, our reconstructed CH_4 emissions increased by 20%, over 90% of which can be attributed to changes in air temperature, precipitation and atmospheric CO_2 concentration. An increasing trend in summer air temperature explained the majority of the climate-related variance".

P5951 L6: "two-dimensional matrices"; it is unclear what the two dimensions of the sensitivity matrices are here. Please clarify.

We have rewritten this sentence as "Then, we computed the average sensitivities in each group, and plotted them as a function of JJA T and P. This gave us two-dimensional matrices of sensitivities".

P5951 L7-L9: Argument is hard to follow, please consider revising.

This is now rewritten as "Grid cells with same JJA T and P conditions typically came from quite different locations in the study domain, thus the resulted averaged sensitivities were not overly influenced by the wetland characteristics of a single region".

P5957 L24: "these sensitivities"; presumably these are climate sensitivities. Please be more specific, given that this is the first sentence in this subsection.

The sentence has been rewritten as "To create a projection of future CH_4 emissions based on the climate sensitivities (Sections 2.4 and 3.2.2), we computed matrices of the sensitivity of aggregate annual emissions to each annual driver as a function of JJA T and P (Fig. 9), similarly to the earlier correlation matrices (Fig. 6)".

P5963 L23-L24: "This is slightly higher than (but within the range of) previous estimates." The two statements are mutually exclusive, please clarify.

We have rewritten this as "This is on the slightly higher end, but still within the range of previous estimates".

P5963 L25: Conclusion 2 is wholly contingent on the model used in this study. The authors should make this clear.

We have rewritten this as "Based on our model, climate change over the last ~ half century has led to a substantial (20%) increase in total emitted CH_4, with increases in air temperature (and associated downward longwave radiation) being the dominant driver".

Technical corrections

Figure 6: The "4" in CH4 not aligned correctly with text.

Fixed

Anonymous Referee #2

In their paper Chen et al. describe the sensitivity of their wetland and methane model to historical and future climate change. Based on observations of wetland maps and methane fluxes they find a model derived increase of methane emissions of 20% over the second half of the 20th century period. While this result itself is not ground breaking, and most probably model dependent, they achieve to incorporate dynamic wetland area changes into their methane estimates, which is rarely done in methane process modelling studies. Hereby also lies the shortage of the study. Methane fluxes are analysed in great detail, but the simulated wetland tile fractions, e.g. changes of wetland area in the future, are not presented. I thus encourage the authors to cover this aspect and suggest a publication of the paper after other minor revisions. The paper is very well organised and written concisely.

We thank the reviewer for the careful reading of the manuscript, as well as his/her insights into the analysis. However, it is important to point out that our model does not include dynamic wetland area. Rather, in our model the wetland tile fraction is fixed, and wetlands are peatlands, which has a fixed area. What does change is the seasonal area of inundation those fractions of our grid cells that are prescribed to be peatland. This is a subtle but important difference.   For this reason, it is incorrect for reviewer to characterize this as "dynamic wetland area". But if the reviewer is referring to inundated area by "wetland area", then we do have these dynamics in the VIC model. Regarding the fact that our results are model-dependent, reviewer #1 also had this concern; we have added an analysis of parameter uncertainty to address this point (see above).   Our responses to other specific comments are included below.

General:

I really like the analysis on methane fluxes and spatial changes for one future projection. As mentioned above I would like to see which part of the methane changes is related to changes in wetland area. Are they spatially or temporally correlated? If precipitation is

the dominant factor for methane emissions in the future, instead of temperature, would this mean wetlands are more susceptible to dryness (on-off state of emissions) and thus larger interannual variability in methane emitting areas and emissions? In addition to mean changes, a paragraph about interannual variability of methane changes would be worthwhile.

We assume by "wetland area" the reviewer is referring to "inundated area" (see above). We have added the analysis of inundation area over the historical period: 1) We added a map (figure 13) showing the changes in inundation area and water table level from each wetland grid cell between the periods 1960-2006 and 2081-2100; 2) We included a paragraph in the manuscript that talks about this change, as well as its possible relations to changes in the methane emitted from the wetland. We also calculated a spatial correlation coefficient between changes in inundation fractions, and changes in methane emitted, to check whether they are spatially correlated.

The discussion of interannual variability in methane emissions is handled with the comments from reviewer #1.

Specific:

p. 5942, l. 10: add CH4 emissions in "... sensitvities of CH4 emissions to air temperature, ..."

The sentence is now rewritten as "We characterized historical sensitivities of annual CH_4 emissions to annual average air temperature, precipitation, incident long- and short-wave radiation, and atmospheric $[CO_2]$ as a function of average summer air temperature and precipitation".

p. 5945, l. 13: typo: Seneviratne

Corrected.

p. 5948, l. 12: What type of plants are simulated by VIC? Is plant productivity dependent on the wetland water table? Are there plant stresses incorporated?

VIC simulates all the MODIS land cover types. When it comes to plants, it does not simulate each type of plant, but only several categories (such as broadleaf evergreen forest, broadleaf deciduous forest, needle leaf evergreen forest, needle leaf deciduous forest, shrubland, grassland, and peatland). Yes, the net primary productivities of these plant categories depend on the wetland water table depth, with an inhibition effect when the water table is above the soil surface (Bohn et al., 2013). We have inserted a statement to this effect into section 2.2.

p. 5949, l. 5: Soil carbon pools normally have turnover times of several centuries. 50 years spinup thus seems to be relatively short. How are they brought into equilibrium? What's the impact on methane emissions?

This is a good point, about which we were not sufficiently clear. Model spin-up consisted of two stages: (1) initialization of carbon pool storages, and (2) 50-year spinup to stabilize moisture and carbon pools. We initialized soil carbon pools via an iterative procedure in which we identified the initial storage that would result in zero net change in carbon storage over the period 1948-1957. Then, to account for the pools' not yet having reached equilibrium with recent Holocene climate, we rescaled all three pool storages by the ratio of observed to simulated total carbon storage across West Siberia, using observations from Sheng et al. (2004). Then we ran the model for 50 years (5 × the decade 1948-1957) to stabilize its moisture and carbon storages. Starting from the model state at the end of this 50-year spin-up, we then performed simulations for 1948-2006. We have added a statement to this effect in Section 2.2.

p. 5949, l. 14: typo : '... expressed as a function ...'

The sentence is now corrected: "Air temperature and longwave radiation were considered together, since downward longwave radiation can be expressed as a function of near-surface air temperature (e.g., Brutsaert, 1975)".

p. 5949, l. 18: typo: '... each year's ratio ...'

This is now corrected as "For annual total precipitation and annual average shortwave radiation, we linearly regressed the annual values, computed each year's ratio of detrended to original annual values, and multiplied all original daily values by that ratio for each day within the year.".

p. 5951, l. 10: typo: '... dominant emission controls'

This is now corrected as "Identifying the dominant emission controls".

p. 5952, l. 20: Please also show a map of modelled changes in lake-wetland fractions over the historical period.

We have now included a map showing the difference of inundation fractions between historical (1960-2006 average) and future (2081-2100) periods (figure 13). We realize that this is not exactly what the reviewer asked for, but we believe that showing the difference between historical and future fits better into the structure of the paper, since we show the differences in correlations between these same two periods in Figure 12, which allows for comparison between areas that got wetter or drier and areas that changed from T- to P- limitation or vice versa.

p. 5953, l. 13: If emissions are strongest in the forest belt: are there forested wetlands present in the model? Or is this a combination of two variables, i.e. forest derived NPP and wetland fraction, that happen to maximize?

The boreal forest belt does contain some forested peatlands, as well as nonforested peatlands and peatlands that contain sparse tree cover. But this is not what we meant. By this statement, we simply mean that peatlands in the boreal forest belt have the highest emissions rates in our model. Our model does not explicitly simulate forested peatlands; peatlands are represented as a combination of shrubby, herbaceous, and moss cover. However, we prescribed LAI with the MODIS MCD15A2 product, and peatlands in the boreal forest belt do have higher LAI values than elsewhere (Fig. 2); thus those peatlands did receive higher labile C inputs than elsewhere. We have added statements to sections 2.2 and 3.1 to clarify these points.

p. 5954, l. 1: This "north"-"south" difference is it because of wetland vegetation type, i.e. sedges versus sphagnum moss, or peat types, i.e. bogs versus fens? What does it mean biogeographically. Please introduce these terms and give a bit more detail.

We apologize, "wetland type" was a poor choice of words here. "Bioclimatic zone" is more appropriate. The north-south difference is simply a result of the calibration in Bohn et al. (2013) achieving a better fit to the observations when a different set of model parameters was applied in the northern half of the West Siberian Lowland domain, following the approximate boundary between the southern/middle taiga and northern taiga/tundra climate zones. To transfer these parameters to the rest of the high latitudes, we chose an LAI threshold to approximate the boundary between these two portions of the boreal forest belt. We have inserted a statement clarifying this point in section 2.2 (where this is first explained), replaced "wetland type" with "bioclimatic zone" on page 5954, and also have added text referring the reader to section 2.2 on page 5954.

p. 5954, l. 25: typo: Table 4, 4th column

This is now corrected as "Emissions from the control runs are shown in Fig. 5b–f. Defining the net impact of a driver as the difference between the historical trend in CH_4 emissions and the trend of the corresponding control run (Fig. 5a and Table 4, 4th column), …".

p. 5963, l. 10: Please cite Stocker et al., 2013 that find a constant feedback climate CH4 factor, albeit an increase in arctic methane emissions in the future. They use CMIP5 simulations paired with a dynamic vegetation model, wetland plant functional types and related methane emissions.

We have modified this sentence: "… (the wetland–climate–CH_4 feedback as discussed by Ringeval et al., 2011, Koven et al., 2011, and Stocker et al., 2013).". Also the reference list is updated to include this paper.

Figure 10: Years on time axis are not nicely spaced.

fixed.

References

Bloom, A. A., Palmer, P. I., Fraser, A., Reay, D. S., and Frankenburg, C.: Large-Scale Controls of Methanogenesis Inferred from Methane and Gravity Spaceborne Data, Science, 327, 322, doi: 10.1126/science.1175176, 2010.

Bohn, T. J., Podest, E., Schroeder, R., Pinto, N., McDonald, K. C., Glagolev, M., Filippov, I., Maksyutov, S., Heimann, M., Chen, X., and Lettenmaier, D. P.: Modeling the large-scale effects of surface moisture heterogeneity on wetland carbon fluxes in the West Siberian Lowland, Biogeosciences, 10, 6559-6576, doi:10.5194/bg-10-6559-2013, 2013.

Bohn, T. J., Melton, J. R., Ito, A., Kleinen, T., Spahni, R., Stocker, B. D., Zhang, B., Zhu, X., Schroeder, R., Glagolev, M. V., Maksyutov, S., Brovkin, V., Chen, G., Denisov, S. N., Eliseev, A. V., Gallego-Sala, A., McDonald, K. C., Rawlins, M.A., Riley, W. J., Subin, Z. M., Tian, H., Zhuang, Q., and Kaplan, J. O.: WETCHIMP-WSL: intercomparison of wetland methane emissions models over West Siberia, Biogeosciences, 12, 3321-3349, doi:10.5194/bg-12-3321-2015, 2015.

Bousquet, P., Ringeval, B., Pison, I., Dlugokencky, E. J., Brunke, E.-G., Carouge, C., Chevallier, F., Fortems-Cheiney, A., Frankenberg, C., Hauglustaine, D. A., Krummel, P. B., Langenfelds, R. L., Ramonet, M., Schmidt, M., Steele, L. P., Szopa, S., Yver, C., Viovy, N., and Ciais, P.: Source attribution of the changes in atmospheric methane for 2006-2008, Atmos. Chem. Phys., 11, 3689-3700, doi: 10.5194/acp-11-3689-2011, 2011.

Slater, A. G., Bohn, T. J., McCreight, J. L., Serreze, M. C., and Lettenmaier, D. P.: A multimodel simulation of pan-Arctic hydrology, Journal of Geophysical Research, 112, G04S45, doi:10.1029/2006JG000303, 2007.

Su, F., Adam, J. C., Trenberth, K. E., and Lettenmaier, D. P.: Evaluation of surface water fluxes of the pan-Arctic land region with a land surface model and ERA-40 reanalysis, *Journal of Geophysical Research: Atmospheres,* 111(D5), D05110, doi: 10.1029/2005JD006387, 2006.

Zhu, X., Zhuang, Q., Chen, M., Sirin, A., Melillo, J., Kicklighter, D., Sokolov, A. and Song, L.: Rising methane emissions in response to climate change in Northern Eurasia during the 21st century, Environmental Research Letters, 6, 045211, doi: 10.1088/1748-9326/6/4/045211, 2011.

Model estimates of climate controls on pan-Arctic wetland methane emissions

X. Chen[1], T. J. Bohn[2], and D. P. Lettenmaier[3]

[1]{Department of Civil and Environmental Engineering, University of Washington, Seattle, WA, USA}

[2]{School of Earth and Space Exploration, Arizona State University, Tempe, AZ, USA}

[3]{Department of Geography, University of California, Los Angeles, CA, USA}

Correspondence to: T. J. Bohn (theodore.bohn@asu.edu)

Abstract

Climate factors including soil temperature and moisture, incident solar radiation, and atmospheric carbon dioxide concentration are important environmental controls on methane (CH_4) emissions from northern wetlands. We investigated the spatio-temporal distributions of the influence of these factors on northern high latitude wetland CH_4 emissions using an enhanced version of the Variable Infiltration Capacity (VIC) land surface model. We simulated CH_4 emissions from wetlands across the Pan-Arctic domain over the period 1948-2006, yielding annual average emissions of ~~35~~36.1±6.7 TgCH_4 y^{-1} for the period 1997-2006. We characterized historical sensitivities of CH_4 emissions to air temperature, precipitation, incident long- and short-wave radiation, and atmospheric $[CO_2]$ as a function of average summer air temperature and precipitation. Emissions from relatively warm and dry wetlands in the southern (permafrost-free) portion of the domain were positively correlated with precipitation and negatively correlated with air temperature, while emissions from wetter and colder wetlands further north (permafrost) were positively correlated with air temperature. Over the entire period 1948-2006, our reconstructed CH_4 emissions increased by 20%, ~~over 90% of which can be attributed to climate change~~changes in air temperature, precipitation and ~~atmospheric CO_2 concentration. An~~the majority of which can be attributed to an increasing trend in summer air temperature ~~explained the majority of the climate-related variance~~. We estimated future emissions in response to 21st Century warming as predicted by CMIP5 model

projections to result in ~~end~~ end-of ~~of~~ century CH$_4$ emissions ~~42~~38-53% higher than our reconstructed 1997-2006 emissions, accompanied by the northward migration of warmer- and drier-than optimal conditions for CH$_4$ emissions, implying a reduced role for temperature in driving future increases in emissions.

1 Introduction

Methane (CH_4) is an important greenhouse gas, with a greenhouse warming potential about 25 times that of CO_2 (IPCC, 2013). Globally, wetlands are the largest natural CH_4 source (Fung et al., 1991; Hein et al., 1997; IPCC, 2013). The strong sensitivity of wetland CH_4 emissions to ambient soil conditions has led to concerns about possible feedbacks to climate change (Gedney et al., 2004; Eliseev et al., 2008). The northern high latitudes contain about one-half of the world's wetlands (Lehner and Döll, 2004) and are experiencing more rapid climate change than elsewhere globally (Serreze et al., 2000; Diffenbaugh and Giorgi, 2012). The potential liberation of vast quantities of carbon from thawing permafrost provides additional impetus to efforts to understand the sensitivity of northern wetland CH_4 emissions to climate change (Schaefer et al., 2011; Koven et al., 2011).

CH_4 emission rates in northern wetlands (which are predominantly peatlands) depend on a number of environmental and climate controls, including soil temperature, water table depth, labile carbon substrate, soil pH, oxidation state, nutrient concentrations, and vegetation composition (Saarnio et al., 1997; Christensen et al., 2003; Zhuang et al., 2004; Riley et al., 2011; Spahni et al., 2011; Glagolev et al., 2011; Lupascu et al., 2012; Levy et al., 2012; Olefeldt et al., 2013; Sabrekov et al., 2014). Many of these factors can interact and compete. For example, Bohn et al. (2007) showed via a process-based model that air temperature and precipitation exert competing influences on (a) water table depth, through winter snow accumulation, spring snow melt, and summer precipitation and evapotranspiration; and (b) metabolic rates, through soil temperature; leading to trade-offs in their influences over emissions. Extreme (limiting) values of one factor can raise the sensitivity of emissions to that factor (Olefeldt et al., 2013). As a result of these interactions, different factors exert dominant controls at different sites (Olefeldt et al., 2013) or time scales (Sabrekov et al., 2014), hindering efforts to constrain model behaviors in the face of sparse observations (Melton et al., 2013). Therefore, isolating those conditions under which different factors dominate or limit the response of wetland methane emissions to climate change would benefit future field campaigns and modeling studies.

Previous attempts to characterize the sensitivities of northern wetland CH_4 emissions to environmental factors have included both data-driven (Bloom et al., 2010; Olefeldt et al., 2013) and process-based modeling (Bohn et al., 2007; Ringeval et al., 2010) approaches.

Data-driven studies have the potential advantages of relative accuracy and simplicity, but can have limited predictive power. For example, Olefeldt et al. (2013) found clear relationships between observed emissions from over 300 high-latitude sites and soil temperature, water table depth, and vegetation composition. However, while these relationships are a crucial step forward in our understanding, ~~these~~ they ~~relationships~~ must be embedded within a process-based model to estimate the aggregate response of northern wetland emissions to a given change in climate, or characterize how these relationships may change with changing climate. Bloom et al. (2010) fit a regression model to observed atmospheric CH_4 concentrations from the Scanning Imaging Absorption Spectrometer for Atmospheric Chemistry (SCIAMACHY; Bovensmann et al., 1999) to observed surface temperatures from the National Center for Environmental Prediction/National Center for Atmospheric Research (NCEP/NCAR) weather analyses (Kalnay et al., 1996) and gravity anomalies from the Gravity Recovery and Climate Experiment satellite (GRACE; Tapley et al., 2004), and found that air temperature exerted the dominant control over high-latitude emissions. Unfortunately, the short (four years) record length and the use of GRACE data as a proxy for near-surface wetland soil moisture suggest that these findings are highly uncertain and limited to the timespan of the satellite datasets used.

Process-based studies potentially have greater predictive power, but their relative complexity may involve highly uncertain parameterizations. For example, Ringeval et al. (2010) found that variations in inundated area contributed 30% to the interannual variability in CH_4 emissions over the latitudes north of 50° N. However, despite the strong emissions observed at non-inundated peatlands throughout the high latitudes (e.g., Saarnio et al., 1997; Panikov and Dedysh, 2000; Friborg et al., 2003; Glagolev et al., 2011), they only considered emissions from inundated wetlands, thus potentially inflating the contribution attributed to inundation. Bohn et al. (2007) accounted for non-inundated emissions, but their study was restricted to a small area in West Siberia. Numerous other process-based studies (using both forward and inverse models) have investigated the response of northern CH_4 emissions to historical or future climate variations (e.g., Chen and Prinn, 2006; Bousquet et al., 2011; Riley et al., 2011; Spahni et al., 2011; Bohn et al., 2013; Zhu et al., 2014; Bohn et al., 2015), but none have attempted to characterize the sensitivities of emissions to climate factors as a function of geographic location, wetland type, or climate conditions.

CH$_4$ emissions are not the only biogeochemical process for which environmental controls have been investigated. Nemani et al. (2003) found that annual net primary productivity (NPP) is limited by temperature and radiation at high latitudes, but by moisture-related factors at lower latitudes. Teuling et al. (2009) and Seneviratne~~Sineveratne~~ et al. (2010) investigated global climate controls on annual evapotranspiration (ET), and found that temperature is the dominant control over northern Eurasia, while precipitation is the dominant control at mid-low latitudes and in northern Canada. These data-driven studies all produced maps of the regions in which various climate factors dominate the flux in question. Such maps are useful in understanding how climate factors interact, which processes are most important, and how these fluxes might evolve under future climate change, particularly in cases where observations are sparse (as is true for CH$_4$ emissions).

In this study, we use a process-based model to characterize the dominant climate drivers of northern high-latitude wetland CH$_4$ emissions, and how they will change with changing climate. We address three questions:

(1) What have been the aggregate long-term CH$_4$ emissions from the Pan-Arctic wetland area over the last 50 years, and how have they changed?

(2) What have been the dominant factor(s) controlling changes in the space-time variability of CH$_4$ emissions over that time period?

(3) How will these conditions be affected by a changing climate over the remainder of the 21st Century?

To investigate these questions, we use an enhanced version of the Variable Infiltration Capacity (VIC) large-scale hydrology model (Liang et al., 1994; Bohn et al. 2013) and the wetland CH$_4$ emissions model of Walter and Heimann (2000). In answering questions (2) and (3), we develop (a) maps of the sensitivities of simulated Pan-Arctic wetland CH$_4$ emissions to various environmental factors, (b) maps of correlations between these factors and CH$_4$ emissions, and (c) empirical estimates of how these sensitivities and correlations depend on climate. These sensitivity maps and climate dependencies provide a basis for projecting future emissions in the region, which we then compare with our VIC model projections to evaluate their ability to capture the effects of underlying processes.

2   Methods

2.1   Spatial Domain

Our study domain is the ~~Pan-Arctic land area, which we define as the~~ global land area north of 45°N (Figure 1a) with slight modifications. ~~It~~Because this region contains all the river basins that drain into the Arctic Ocean, we will refer to it as the "Pan-Arctic" hereafter, as in Slater et al. (2007). Our domain boundaries are as in the TransCom project (Gurney et al., 2000), except that we exclude Greenland. We also include southern Russia and the permafrost part of Tibet. We divided the domain into 3775 100-km equal-area EASE grid cells (Brodzik and Knowles, 2002).

Our domain includes three major wetland areas (Lehner and Döll, 2004; Tarnocai et al., 2009; Figure 1b): the West Siberian Lowland (WSL), which we define as the region from 55° to 75° N and 60° to 90° E; Scandinavia (55°-75° N and 15°-45° E); and the Hudson's Bay Lowland (HBL), which we define as the region from 45° to 60° N and 75° to 100° W. There are also many smaller wetlands distributed over the domain. The vast majority of the domain's wetlands are peatlands, which are reservoirs of organic carbon (Tarnocai et al., 2009), and have the potential to produce huge fluxes of carbon (CO_2 or CH_4) to the atmosphere. Forests cover about 23% of the total land area of our study domain, as evidenced by the belt of high values of leaf area index (LAI) between about 55˚ and 65˚N (Myneni et al., 2002; Figure 1c).

Our domain ~~covers~~ includes essentially the entire northern hemisphere permafrost land area, aside from a few high altitude areas (Figure 1d; see also Brown et al., 2014). Within the permafrost areas, deep soil temperatures are generally below 0°C for successive years, which restricts biological methanogens. However, during summer, the active layer (seasonally thawed) provides a suitable environment for CH_4 production.

2.2   Model Framework

We used a modified version of the Variable Infiltration Capacity (VIC) version 4.1.2 (Liang et al., 1994; Bohn et al., 2013) that simulates carbon fluxes as well as the hydrologic processes represented in the standard version of the VIC model. The VIC model resolves the soil moisture and temperature profiles through a coupled water-energy balance scheme that accounts for cold-climate processes such as soil freeze-thaw and the insulating effects of organic soils. We provide here a brief description of the model features related to wetland

1   process. The main enhancement in the version of VIC we used is a module for calculating the

2   carbon inputs into the ecosystem, which is the substrate source of biogeochemical processes

3   that produce CH_4. Within each grid cell the model represents multiple land cover "tiles". This

4   modified version of VIC also represents lakes and wetlands as described in Bohn et al.

5   (2013). Each grid cell in the study domain is assumed to be composed of a lake-wetland tile

6   and an upland portion (that may contain several different land cover tiles). The lake-wetland

7   tile contains peatlands of fixed area, within which a time-varying portion may be seasonally

8   inundated, and which may contain a permanent lake. Peatlands, which are are modeled as a

9   mix of moss and shrubs, are allowed to emit CH_4, subject to oxidation above the water table,

10 but lake CH_4 emissions are set to zero. The water table depth within peatlands follows a

11 distribution derived from assumed microtopography. ~~Peatlands are modeled as a mix of moss~~

12 ~~and shrubs.~~ Net primary productivity (NPP) within ~~the~~ peatlands experiences inhibition when

13 the water table is above the soil surface. More details of the lake-wetland continuum are

14 included in Bohn et al (2013).

15 Permanent lakes were prescribed using the Global Lakes and Wetlands data set (GLWD) of

16 Lehner and Döll (2004). Wetland areas were taken in most cases from the union of wetland

17 classes from the GLWD and wetland pixels from the MODIS plant functional type dataset

18 MCD12Q1 (Friedl et al., 2010). However, in regions where the GLWD delineated wetland

19 classes as 25-50% and 50-100% (occurring in Alaska and Canada) we defined wetlands as

20 pixels with soil organic carbon content above 70% from the Northern Circum-Polar Soil

21 Carbon Database (Tarnocai et al., 2009). 2049 of the domain's 3775 cells contain wetlands

22 (lake-wetland fractions shown in Figure 1b).

23 The enhanced VIC model is linked to the Walter and Heimann wetland CH_4 emissions model

24 (Walter and Heimann, 2000), as described in Bohn et al. (2013). The Walter and Heimann

25 CH_4 model takes the water table depth distribution, soil temperature profile and net primary

26 productivity (NPP) generated by VIC to calculate a distribution of CH_4 emissions rates. The

27 model assumes that labile carbon leaks into the soil through plant roots in proportion to NPP,

28 and is converted to CH_4 through anaerobic respiration of methanogens as a function of the

29 soil thermal and moisture conditions.

30 ~~We calibrated t~~The combined VIC and CH_4 models were calibrated over West Siberia in

31 Bohn et al. (2013), and we adopted the median parameter values from the distributions from

32 that study (Table 1) for our primary simluations. In Bohn et al. (2013), two parameter sets

were optimized for the West Siberian Llowlands: "south" (primarily within the forest belt, or taiga) and "north" (primarily tundra). These parameter sets only corresponded to broad geographic regions, rather than to specific types of wetlands such as bogs or fens. To extend these parameter sets across our entire domain, we assigned the "south" parameter set to grid cells with July LAI higher than 4, and the "north" parameter set to all other grid cells.

LAI data were taken from the MODIS MCD15A2 data set (Myneni et al., 2002) for the period 2002-2010. We used the mean seasonal cycle for this period repetitively for every year in our simulation period. Soil parameters were taken from Su et al. (2006).

The primary meteorological forcings used to drive the VIC include 3-hourly precipitation, air temperature, wind speed, downward shortwave and longwave radiation. These data were obtained from Sheffield et al. (2006) at 0.25x0.25 degree spatial resolution, which we regridded to 100 km EASE-grid. Atmospheric CO_2 concentration data were taken from Bohn et al. (2013).

2.3 Simulations

Our historical simulation period was 1948-2006. Model spin-up consisted of two stages: (1) initialization of carbon pool storages, and (2) a 50-year spinup to stabilize moisture and carbon pools. We initialized soil carbon pools via an iterative procedure in which we identified the initial storage that would result in zero net change in carbon storage over the period 1948-1957. Then, to account for the pools' not yet having reached equilibrium with recent Holocene climate, we rescaled all three pool storages by the ratio of observed to simulated total carbon storage across West Siberia, using observations from Sheng et al. (2004). We firstThen we ran the model for 50 years (5 × the decade 1948-1957) to stabilize its moisture and carbon storages. Then sStarting from the model state at the end of this 50-year spin-up, we then performed simulations for 1948-2006.

To isolate the effects of various climate factors that drive the variability in CH_4 emissions, we performed five control experiments in which we removed trends (at each grid cell) in one or more variables (air temperature and longwave radiation; precipitation; air temperature, longwave radiation and precipitation; atmospheric CO_2 concentration; and solar radiation)

during the period 1960-2006. Air temperature and longwave radiation were considered together, since downward longwave radiation can be expressed <u>as</u> a function of near-surface air temperature (e.g., Brutsaert, 1975). For air temperature and longwave radiation, we linearly regressed the annual values over time and removed cumulative changes due to the trend since 1960 from each subsequent year. For annual total precipitation and annual average shortwave radiation, we linearly regressed the annual values, computed each year's ~~the~~ ratio of detrended to original annual values, and multiplied all original daily values by that ratio for each day within the year. For detrended atmospheric CO_2, we used the 1960 concentration level for the entire period 1960-2006. Trends in the forcing variables were removed in cases when the trend wa significant at the 0.05 level. At the 0.05 significance level, the entire domain experienced increasing trends in air temperature (0.0322 K y^{-1}), precipitation (0.5183 mm y^{-1}), [CO_2] (1.4009 ppm y^{-1}), and downward longwave radiation (0.0670 W $m^{-2} y^{-1}$), and a decreasing trend in downward shortwave radiation (-0.0385 W $m^{-2} y^{-1}$), which is consistent with Fang et al. (2009) (Table 2).

Using these historical and control forcings, we designed six experiments to investigate the impact of historical climate change on the wetland CH_4 emissions:

  (1) R01: Historical simulation, driven by historical forcings;

  (2) R02: Air temperature and longwave radiation (TLW) control run, using detrended air temperature and longwave radiation;

  (3) R03: CO_2 control run, using the 1960 CO_2 level;

  (4) R04: TLW and precipitation (TLWP) control run, using detrended air temperature, detrended longwave radiation, and detrended precipitation;

  (5) R05: Precipitation (P) control run, using detrended precipitation;

  (6) R06: Shortwave radiation (SW) control run, using detrended shortwave radiation.

2.4   Sensitivities to Climate Drivers as a Function of Climate

We defined the sensitivity coefficients (α) of CH_4 emissions to long-term changes in the driver variables as the partial derivatives:

$$\alpha_p = \frac{dCH_4}{dP} \quad (\mathrm{gCH_4 \cdot m^{-2} \cdot year^{-1} \cdot mm^{-1}})$$

$$\alpha_{TLW} = \frac{dCH_4}{dT_{air}} \quad (\mathrm{gCH_4 \cdot m^{-2} \cdot year^{-1} \cdot K^{-1}})$$

$$\alpha_{CO2} = \frac{dCH_4}{d[CO_2]} \quad (\mathrm{gCH_4 \cdot m^{-2} \cdot year^{-1} \cdot ppm^{-1}})$$ [1]

$$\alpha_{SW} = \frac{dCH_4}{dSW} \quad (\mathrm{gCH_4 \cdot m^{-2} \cdot year^{-1} \cdot (W/m^2)^{-1}})$$

Where the total change in annual methane emissions due to climate change $\Delta CH_4 = \alpha_P \times dP + \alpha_{TLW} \times dT_{air} + \alpha_{CO2} \times dCO_2 + \alpha_{SW} \times dSW + interaction$. The CH_4, T, $[CO_2]$ and SW values in this relationship were ~~taken at prescribed to~~ annual average~~d~~ values, while P was ~~taken as~~ annual total precipitation ~~in the grid cell~~.

We computed the sensitivity coefficients at each grid cell by first computing the timeseries of differences between the historical and control emissions, and then performing a linear regression between the differences in CH_4 and the differences between historical and detrended values of the driver variable. We then created maps of these sensitivities. To characterize the dependence of these sensitivities on climate, we divided the domain's grid cells into groups by their 46-year (1961-2006) average historical JJA T and JJA P, in increments of 2 °C and 20 mm, respectively~~.~~ (JJA T and P were chosen as independent variables ~~with which to~~ for purposes of characterizing~~e~~ sensitivities ~~instead of~~ rather than annual average T and P because the majority of annual CH_4 emissions occur during the growing season~~, such that annual T and P explain less of the variance in annual CH_4 emissions than JJA T and P do~~). Then, we computed the average sensitivities in each group, and plotted them as a function of ~~summer (JJA)~~ PT and ~~summer T~~P. This gave~~giving~~ us two-dimensional matrices of sensitivities. ~~Most groups contained sensitivities from 5-20 grid cells dispersed across the domain, so that the resulting averages~~ Grid cells with the same ~~summer~~JJA T and P conditions~~s~~ could come from quite different locations in the study domain, thus the resulting~~ed~~ averaged sensitivities were not overly influenced by the characteristics of a single region.

2.5 Identifying the Dominant Emissions Controls

We calculated the correlation coefficients between the time series of CH_4 emissions and the various drivers at each grid cell, giving us a map of dominant controls (those with the highest correlations) across the domain. Similarly to the sensitivities in section 2.4, we created 2-dimensional matrices of correlations as a function of JJA T and JJA P.

2.6 Future Projections

We generated two future projections of CH_4 emissions over the period 2007-2106: a process-based projection, in which we ran our modeling framework with future meteorological forcings; and a sensitivity-based projection, in which we applied the four sensitivity coefficients computed in section 2.4 to projected future forcings. To generate meteorological forcings for the future projections, we computed the monthly changes in meteorological forcings from the CCSM4 RCP4.5 projection (which falls near the middle of the set of all CMIP5 RCP4.5 projections) over the period 2007-2106, relative to the period 1996-2005, and applied these changes to the Sheffield et al. (2006) meteorology.

Based on the sensitivity matrices, and given a reference climate condition and corresponding CH_4 emission rate, we can derive the projected emission rate via

$$CH_4(t+1) = \overline{CH_4}(t) + \alpha_P\big(\bar{T}(t), \bar{P}(t)\big) \times \big(P(t+1) - \bar{P}(t)\big) + \alpha_{TLW}\big(\bar{T}(t), \bar{P}(t)\big) \times$$
$$\big(T(t+1) - \bar{T}(t)\big) + \alpha_{CO2}\big(\bar{T}(t), \bar{P}(t)\big) \times \big(CO_2(t+1) - \overline{CO_2}(t)\big) \qquad [2]$$

where t is the year; $\overline{CH_4}(t)$, $\bar{T}(t)$, $\bar{P}(t)$, and $\overline{CO_2}(t)$ are the average values of annual CH_4, JJA T, JJA P, and [CO_2] for the current grid cell over the last 10 years, and the coefficients are those defined in equation [1]. Here we assume that interactions among the individual climate forcings are negligible. We check this assumption in section 3.2.1. We also assume that, as a grid cell's average T and P change, its sensitivities to drivers will evolve to resemble the current sensitivities of cells at the new (T, P) coordinates. We discuss the validity of this assumption in Section 4.2.

2.7 Parameter Uncertainty

Unless otherwise stated, oOur baseline simulations used the median parameter values of Bohn et al. (2013) as described in section 2.2. However, to assess the effects of parameter uncertainty on our results, we also generated an ensemble of 18 simulations using randomly

sampled parameter values from the posterior distributions of Bohn et al. (2013) (Table 1). The parameters that we examined included r_0^* (the reference CH_4 production rate per unit annual average LAI), xvmax (the maximum CH_4 oxidation rate), rkm (the Michaelis Menten constant), rq_{10} and oxq_{10} (the Q_{10} values for the temperature dependencies of the CH_4 production and oxidation rates, respectively), and tveg, a dimensionless integer value ranging from 0 to 15 that indicates the strength of plant-aided transport. The posterior distribution of tveg, which was held constant at a value of 12 in Bohn et al. (2013), was determined via Bayesian estimation from an ensemble of 3000 simulations that randomly sampled values of tveg across the range 0 to 15 and sampled values of all other parameters from their posterior distributions, in comparison with the observations of Glagolev et al. (2011). We did not vary the parameter pox, which determines the fraction of CH_4 oxidized in the root zone, as variations in tveg can compensate for variations in pox. Instead, we held pox constant at a value of 0.5, as in Walter and Heimann (2000) and Bohn et al. (2013). To account for uncertainty in our estimate of the border between the "south" and "north" regions, we performed two additional simulations, in which the entire domain used either the median "south" parameter set or the median "north" parameter set ("all-south" and "all-north", respectively). Adding these two simulations to our ensemble resulted in a total of 20 simulations. For each of these ensemble members, we constructed a distinct set of sensitivity matrices and created a sensitivity-based projection.

3   Results

3.1   Historical Simulation

Before examining simulated CH_4 emissions, we first evaluated model performance in simulating the environmental factors that are relevant to CH_4 emissions. The spatial distribution of simulated inundation extents was similar to that of the Surface Water Microwave Product Series ("SWAMPS") remote sensing inundation product of Schroeder et al. (2010), with high concentrations in the WSL, Scandinavia, the HBL, and western Canada (Figure 2a,b). VIC's inundated extent was biased low in western Canada, at about half the area given by SWAMPS.

To evaluate our simulated soil temperatures, we compared the distribution of continuous and discontinuous permafrost from the Circum-Arctic Map of Permafrost and Ground-Ice

1 Condition (CAPGIC) map (Brown et al., 2014; Figure 2c) with the VIC-simulated active

2 layer depth (ALD) in the permafrost area (Figure 2d). The spatial distribution of VIC's ALD

3 was similar to the distribution of permafrost. An ALD of 1m is an approximate threshold for

4 "continuous permafrost" in the Brown et al. (2014) map.

5 We compared the simulated NPP distribution (Figure 2e) with the MODIS MOD17A3 NPP

6 product (Running et al., 2004) (Figure 2f). Model results and MODIS patterns matched

7 reasonably well (spatial correlation 0.87), with ~~high~~ slight (about 6%) overestimation of NPP

8 in the boreal forest band between 55° and 65° N latitude. ~~VIC slightly overestimated NPP in~~

9 ~~the boreal forest (Figure 2g): for NPP values less than about 200 g C m^{-2} y^{-1}, simulated values~~

10 ~~(mean of 105 g C m^{-2} y^{-1}) were within 3% of observed (mean of 108 g C m^{-2} y^{-1}), but at higher~~

11 ~~values, simulated values (mean of 392 g C m^{-2} y^{-1}) were biased by about 6% high relative to~~

12 ~~the observed mean of 370 g C m^{-2} y^{-1}.~~

13 The spatial distribution of simulated average annual CH_4 emissions over the period 1960-2006

14 (Figure 3) was similar to the distribution of wetlands (Figure 1b), with notable concentrations

15 in the WSL, Scandinavia, the HBL, and southern Canada. However, emissions were strongest

16 in the boreal forest belt between 55° and 65° N latitude, as a consequence of warmer

17 temperatures, greater inputs of labile carbon (due to the higher rates of NPP there; see Figures

18 2e,f), and the more productive "south" CH_4 parameter set that we used there. As an aside, the

19 higher NPP values in the boreal forest belt do not necessarily imply that the peatlands there

20 are forested, although some peatlands there do contain substantial numbers of trees (~~. T~~the

21 VIC model does not distinguish between forested and non-forested peatlands).

22 We evaluated our simulated CH_4 emissions over three subdomains: the WSL, the HBL, and

23 the high latitudes of the western hemisphere. Over the WSL, we compared our simulations

24 with the estimate of Glagolev et al. (2011), which is based on in situ observations of mire

25 landscape CH_4 emissions during 2007-2010 (Figure 4). While our model tended to

26 overestimate emissions in the middle of the domain, it captured the general north-south

27 gradient in emissions. As to the total emission from the WSL area, Glagolev et al. estimated

28 3.91±1.29 TgCH$_4$ y^{-1}, as compared with our estimate of 7.12 TgCH$_4$ y^{-1}. Our result here is

29 also considerably higher than the estimate of Bohn et al. (2013) of 3.65 TgCH$_4$ y^{-1}, primarily

30 because we (a) replaced that study's WSL-specific peatland maps (Sheng et al, 2004; Peregon

31 et al., 2008), with the GLWD wetland map (Lehner and Döll, 2004), which attributes

32 substantially higher wetland fractions to the region between 63° and 66° N latitude than the

WSL-specific maps do; (b) we replaced the WSL-specific assignment of "north" and "south" CH_4 parameter sets by ~~wetland type~~bioclimatic zone with the more general criterion of July LAI > 4 (section 2.2), which extended the region of more productive wetlands ("south" parameters) slightly further northward; and (c) used the meteorological forcings of Sheffield et al. (2006) instead of those of Adam et al. (2006). However, our estimate is within the range of estimates from inversions over the WSL, which range from 3.08 $TgCH_4$ y^{-1} (Kim et al., 2011) to 9.80 $TgCH_4$ y^{-1} (Schuldt et al., 2013; Winderlich, 2012).

CH_4 emissions over the HBL have been estimated by Pickett-Heaps et al. (2011) as 2.3±0.3 $TgCH_4$ y^{-1} during 2004-2008. Our estimate for the same region is 3.11±0.45 $TgCH_4$ y^{-1}. Although larger than the Pickett-Heaps estimate, it is almost identical to the estimate of 3.1±0.5 $TgCH_4$ y^{-1} by Zhu et al. (2014).

Several studies have estimated total CH_4 emissions from all northern wetlands (Table 3), giving a range of 20-55 $TgCH_4$ y^{-1} over similar domains. Our model gives an estimate of 35.0 $TgCH_4$ y^{-1} during 1997-2006. This result is within the range of estimates from studies since 1990s, and is closer to some of the more recent results, e.g. 34±13 $TgCH_4$ y^{-1} from Chen and Prinn (2006) and 38.1-55.4 $TgCH_4$ y^{-1} from Zhu et al. (2014). The difference is well within the uncertainty range ascribed to most previous estimates.

3.2 Sensitivity to Climate Factors

3.2.1 Historical Trends

Over the entire Pan-Arctic domain, CH_4 emissions increased substantially over the period 1960-2006, with a trend of 0.158 Tg CH_4 y^{-1} (Figure 5a and Table 4, 4th column). Emissions from the control runs are shown in Figure 5b-f. Defining the net impact of a driver as the difference between the historical trend in CH_4 emissions and the trend of the corresponding control run (Figure 5g and Table 2, 4th column), we can see that air temperature and longwave radiation (TLW) had the largest impact on emissions (0.104 Tg CH_4 y^{-1}, or 66% of the historical trend), followed by CO_2 (0.030 Tg CH_4 y^{-1}, or 19%) and precipitation (0.015 Tg CH_4 y^{-1}, or 10%). The combined impact of TLW and P (TLWP), at 0.115 Tg CH_4 y^{-1}, is slightly less than the sum of the impacts of TLW and P separately (0.119 Tg CH_4 y^{-1}), implying that these two drivers acted in opposition to each other to some extent, but also indicating that the interaction between T and P was a relatively small effect. Locally, the

1 effects of precipitation were often larger than those of CO_2, but these effects largely canceled

2 over the domain.

3.2.2 Sensitivity as a Function of Climate

4 The sensitivities of wetland CH_4 emissions to the climate factors we investigated varied in

5 space or time, and were strongly influenced by climate conditions. In Figure 6a, which shows

6 the distribution of spatial average annual CH_4 emissions as a function of 10-year average JJA

7 T and P, maximum CH_4 emissions occur along a "ridge" of slope 13 mm K^{-1} for JJA T values

8 above 285 K and JJA P values above 120 mm. Consequently, increasing one factor (P or T)

9 while holding the other factor constant may cause CH_4 emissions to increase or decrease,

10 depending on the current climate state of the wetland. Under relatively cold or dry conditions,

11 emissions tend to increase with increasing T and P. But at high P values, emissions decrease

12 with increasing P, due to the inhibition of NPP under inundated conditions in the VIC model

13 (Bohn et al., 2013). At high T values, emissions decrease with increasing T, due to increased

14 oxidation of CH_4 as higher evaporation rates draw down the water table (Bohn et al., 2007).

15 Temporal correlations between historical annual CH_4 emissions and the three most important

16 climate drivers (JJA T, JJA P, and JJA CO_2) were fairly consistent with this pattern (Figure 6b

17 – d). Correlations between annual CH_4 emissions and JJA T (Figure 6b) were highest when

18 JJA T is to the left of (colder than) the ridge of maximal emissions in Figure 6a, and lowest

19 (negative, in fact) to the right of (warmer than) the ridge. Similarly, correlations with JJA P

20 were highest below (drier than) the Figure 6a ridge and lowest (negative) above (wetter than)

21 the ridge, although this pattern broke down for JJA T below 285 K, where temperature

22 limitation dominated the response and correlations with JJA P were only weakly positive or

23 negative. Correlations with JJA CO_2 were moderately positive at all but the most extreme

24 JJA T and P conditions, implying that CH_4 emissions generally benefit from CO_2 fertilization,

25 via increased input of carbon substrate into the soil.

26 These differing responses of wetland CH_4 emissions to climate factors displayed strong

27 geographic patterns, as a function of local climate (Figure 7). In Figure 7a, the ensemble

28 median correlations between CH_4 and JJA T are represented on a blue (positive) to yellow

29 (negative) color gradient. Similarly, correlations between CH_4 and JJA P are represented on a

30 red (positive) to green (negative) color gradient. Therefore blue indicates a strong positive

31 temperature control on CH_4 emissions (T+), and this can be thought of as too cold for

maximum emissions; yellow indicates a strong negative temperature (T-) control (too warm); green indicates a strong negative precipitation ("P-") control (too wet), and red indicates a strong positive precipitation ("P+") control (too dry). In general, northern cells ~~are~~ were T+ dominated (blue), due to the low summer air temperatures that they experience. These blue regions corresponded approximately to the distribution of permafrost (Figure 1d). ~~As we move~~Moving southward, emissions ~~become~~ became P+ dominated (red). Southern West Siberia is relatively dry and warm, thus showing both P+ and T+ controls (orange). But in the northernmost regions of Alaska and Canada (where inundation fractions ~~are~~ were high, see Figure 2b), we saw predominantly P- control (green). Comparison of this figure with Figure 2b also shows that P+ and T+ (orange) areas ~~are~~ were associated with smaller inundated area fractions and warmer temperatures, due to deeper water tables and greater oxidation rates.

Parameter-based uncertainties in the correlations (Figure 7b), expressed as the range of correlations across the ensemble, were generally small (< 0.3) in both the T and P dimensions, except for P- limited (green) regions in northeastern Canada and central Tibet and the northern portion of the T+ limited region in north-central Canada. The general pattern of P+ limitation in the southern reaches of the domain and T+ limitation in much of the northern reaches of the domain appeared in all ensemble members.

Correlations between emissions and drivers tell us which driver is most influential at a given location. However, the sizes of the correlations are affected by both the relative sensitivities of emissions to the drivers and the relative amplitudes of the drivers' signals. It is therefore useful to consider the sensitivities alone. Sensitivities of annual emissions to the three main drivers (JJA T, JJA P, and JJA CO_2) ~~are~~ were markedly higher outside the continuous permafrost zone than within it (Figure 8). To first order, the explanation for this pattern is the general insensitivity of CH_4 emissions to all drivers at low temperatures, evident in Figure 6a. Nevertheless, there ~~are~~ were important differences among the distributions; e.g., emissions in eastern Canada and eastern Siberia showed strong sensitivity to T, but weak sensitivity to P and CO_2. Spatial correlations between these sensitivities and various hydrologic and ecological terms, listed in Table 5, give some indication of which processes ~~are~~ were most influential. The sensitivity of CH_4 emissions to JJA T (Figure 8a) ~~is~~ was most highly correlated (r = 0.30) with April-May snow water equivalent (AM SWE), which ~~would be~~is consistent with a lack of water limitation, due to larger spring snowpacks leading to wetter summer conditions. Similarly, the sensitivity of emissions to P (Figure 8b) ~~is~~ was larger in

absolute magnitude (positive or negative) where temperatures ~~are~~ were warm, allowing for a higher (temperature-dependent) CH_4 production rate to be affected more dramatically by oxidation under drier conditions and reduced carbon input under wetter, more inundated conditions. The lack of strong correlations between the sensitivity to P and the various environmental factors in Table 5 may be the result of relatively high spatial heterogeneity in P and wetland moisture conditions (e.g., inundation), in comparison with that of T, leading to more "noise" in the relationships between them. Finally, the sensitivity of emissions to CO_2 (Figure 8c) ~~is~~ was most strongly correlated (r = 0.45) with NPP (Figure 2f), which is consistent with the relationship between rates of carbon input into the soil and NPP in the model of Walter and Heimann (2000). Because relatively warm conditions and high NPP are associated with boreal forests, the geographic distributions of sensitivities to all factors also ~~bear~~ bore strong similarity to the distribution of boreal forest.

3.3   Process- and Sensitivity-Based Projections

To create a projection of future CH_4 emissions based on the climate~~these~~ sensitivities, we computed matrices of the sensitivity of aggregate emissions to each driver as a function of JJA T and P (Figure 9a,c,e), similarly to the earlier correlation matrices (Figure 6). To ensure that sensitivities exist for all possible future combinations of JJA T and P in the projection, we filled gaps in the matrices via a 3 row x 3 column window with a Gaussian kernel with $\sigma=1$. Similar to the correlation matrices discussed in section 3.2.2, the sensitivities to JJA T, JJA P, and [CO_2] all exhibited maximum values along a diagonal "ridge" for T > 285 K and P > 120 mm (which correspond to the climate conditions in which boreal forest is found). For the sensitivities to JJA T and [CO_2], the ridges had similar slopes of approximately 30 mm K^{-1}. Sensitivities to JJA T were negative for P < 50 mm and 285 K < T < 291 K, due to increasing CH_4 oxidation above the water table with increasing temperature. In contrast, the ridge of maximum sensitivities to JJA P had a lower slope of about 12.5 mm K^{-1}, with a region of negative sensitivities for P > 190 mm and 287 K < T < 293 K, due to reduced productivity under inundated conditions. Again, sensitivities to all drivers were nearly zero for JJA T < 285 K, due to the non-linear temperature dependence of CH_4 production as well as the tendency for wetlands in that temperature range to be less productive (and therefore use the less productive "north" parameter set). Uncertainty in the methane model parameters (across the ensemble of random parameter combinations) led to a wide range of sensitivity values (Figures 9b, d, and f). However, the contours of the matrices of the individual ensemble

members had similar shapes, so that regions of higher or lower sensitivities occurred in similar locations in climate space.

The ensemble of sensitivity-based projections, created by applying these sensitivity matrices to meteorological forcings based on the CCSM4 RCP4.5 projection over the period 2006-2106, yielded a similar trajectory of CH_4 emissions to the projection from our process-based model (Figure 10). Both the process-based (black) and median sensitivity-based (blue) projections agreed that emissions will initially remain relatively constant from 2007 to 2026 (in response to relatively little trend in air temperatures over the period; Figure 10b) and then resume their increase. For the period 2056-2065, the process- and median sensitivity-based projections reached 46.1 and 43.4 Tg CH_4 y^{-1}, respectively (132% and 124%, respectively, of the 1997-2006 level). By the end of the century (2096-2105), they reached 50.1 and 48.3 Tg CH_4 y^{-1} (142% and 138%, respectively, of their 1997-2006 levels). Uncertainty in the methane model parameters led to a range of 39 to 57 Tg CH_4 y^{-1} in sensitivity-based end-of-century emissions at the 95% confidence level. However, the other members of the uncertainty ensemble followed ~~similar~~ trajectories that were similar to the median sensitivity-based projection over the course of the century, resulting in increases of 38 to 53% over their 1997-2006 levels.

While the two projections agreed on long-term behavior, their year-to-year variability disagreed at times, with the median sensitivity-based projection sometimes anti-correlated with the process-based projection. This is likely due to our construction of average sensitivities over all grid cells having similar climate conditions, which ignored the influence of local land cover, topography, and soils. Thus, during some years in some grid cells, our sensitivity matrices may have indicated a sensitivity of opposite sign to that of the process-based model, due to the grid cell's "ridge" of maximum emissions occurring in a different location in T-P space than in the domain-average matrix. Nevertheless, the general agreement in the long-term, domain-wide behavior implies that the sensitivity-based method captured the aggregate response of wetland CH_4 emissions to climate reasonably well.

Geographically, the regions of largest increases in emissions during the next century were in the boreal forest belt (Figure 11a,c). This behavior was fairly consistent across the ensemble of methane parameter sets, with the exception of uncertainties > 30% of the median in southern Canada and northwestern Siberia (Figure 11b). ~~, but the~~These increases in emissions began at the southern edge of the domain and spread northward over time. ~~This northward~~

18

migration of strong emissions ~~corresponded~~ corresponding to a northward shift in the types of controls exerted by climate factors, as shown in Figure 12. Between 1997-2006 and ~~2026~~2096-~~2035~~2105, areas of P+ control (red and pink) migrated northward by ~~5-10~~10-20° of latitude, into territory that was previously under T+ control (blue) (Figure 12, left~~a,b~~). In other words, wetlands between 55 and 65° N latitude that were previously colder than optimal experienced warming without a sufficient corresponding increase in precipitation, leading to their becoming drier than optimal, and increasing their positive response to increases in precipitation. Other regions of historically T+ control with large lake areas (e.g., Finland and Northern Canada) were replaced by P- control (green) as they warmed. ~~Then, over the remainder of the century, areas of T-, P+ control (orange) migrated northward by 5-10° of latitude, into territory that was previously under P+ control (red) (Figure 12c,d). Thus, wetlands between 50 and 60° N latitude became increasingly warmer (and drier) than optimal, giving them a negative response to further increases in temperature.~~ These patterns were robust across the parameter uncertainty ensemble, with large uncertainties primarily confined to northeastern Canada (Figure 12 right).

To investigate the role of ~~dynamic wetland~~ inundat~~ion~~ed area in the interannual variation of methane emissions, we calculated the changes in inundat~~ion~~ed frac~~tion~~ (Figure 13a-c) and ~~changes in the~~ mean water table levels (Figure 13d-f) ~~from~~ of the process-based projection between the periods 1960-2006 ~~period to~~and 2081-2100 ~~period~~. The large areas of drying (reduced inundated area and falling water tables ~~levels~~) in southern Canada and Alaska in Figures 13c and 13f are consistent with the increase in the extent of P+ limited (red) wetlands in those same places over the 21st century shown in Figure 12.

4   Discussion

4.1   Historical Climate Controls on CH$_4$ Emissions

Our analysis indicates that summer air temperature increases explain almost two-thirds of the long-term trend in CH$_4$ emissions over the last-half century over the pan-Arctic domain. Precipitation ~~has~~ had a smaller net effect (it explains only 10% of the long-term trend), but

this is due in part to spatial heterogeneity in the historical trends of P and their effects on CH_4, leading to partial cancellation over pan-Arctic domain. Nevertheless, the dominant role of air temperature in the pan-Arctic is not entirely surprising, given that the region is generally cold, leading to temperature limitation on metabolic rates. Our map of the historical controls on emissions (Figure 7) corroborates this notion, since most of the region has historically been T+ limited. This finding is largely consistent with Bloom et al. (2010), who also found that air temperature was the dominant factor controlling CH_4 emissions at high latitudes. However, our finding of strong P+ limitation in the band between 50 and 60 °N (Figure 7) is at odds with Bloom et al. (2010). This discrepancy may be due to a lack of variability in GRACE observations there (Bohn et al., 2015) or the inability of the global linear regression used by Bloom et al. to capture the location- and climate- dependent sensitivities accounted for by process-based models and the sensitivity-based approach that we have used here.

Within the pan-Arctic domain, we found strong geographic patterns in climate controls on CH_4 emissions. Similar (observation rather than model-based) analyses have been performed on NPP (Nemani et al., 2003) and ET (Teuling et al., 2009). Our study shares some similarity in conclusions. For example, these studies show that CH_4, NPP and ET are all T+ controlled around Hudson Bay and in Scandinavia, and P+ controlled in the wetlands of southwestern Canada. This is not surprising, because NPP and ET are both tightly linked with CH_4 production: NPP determines how much carbon can be converted to CH_4, while ET is positively correlated with soil moisture content, as is the CH_4 emission rate. In the WSL, the wetlands in the south are P+ and T- ~~limited~~controlled, suggesting that this area is much drier than the north, with more CH_4 emitted as the water tables are drawn down during summer (Bohn et al., 2007). NPP in this southern area is in transition from T limited to P limited (Nemani et al., 2003), which is consistent with CH_4. In a recent process-based study, Liu et al. (2015) also found that ET in southern Siberia is P+ limited.

Despite their similarities, there are some differences in the spatial distributions of controls between our and previous studies. In ~~our~~ Nemani et al. (2003), NPP over northern Europe and West Siberia is almost entirely limited by temperature and radiation, while in our results, CH_4 is P+ limited over a considerable area. This is due in part to the nearly negligible role shortwave radiation plays in CH_4 emissions (Figure 5); in part to the drier optimal soil moisture conditions for upland vegetation (included in the Nemani et al. NPP analysis), relative to wetland plants (which we focus on here); and in part to the rapid drop in CH_4

emissions as the water table is drawn down beyond a few cm. Similarly, the area of P+ limitation of ET in Western Canada in Teuling et al. (2009) is smaller than the area of P+ limitation of CH_4 emissions in our study. This can also be explained by the presence of forested uplands in this area, where the moisture deficit in upper soil layers from low precipitation is partly compensated by water extracted from deeper soils. Thus, only those places with considerable shortage of water will show up as P+ in the Teuling et al. ET map.

The validity of our results depends on ~~the validity of~~ our model's temporal behavior, which is subject to both model uncertainty and parameter uncertainty. Verification opportunities include in situ observations, and atmospheric model inversions. Both are problematic, due to the ~~Given the~~ paucity of long in situ observational records in the first case and the errors to which inversions are subject in the second (~~demonstrated in~~see Bohn et al., 2015)~~, it can be difficult to evaluate temporal behavior at large scales~~. Nevertheless, in Bohn et al. (2015), the interannual variability of our modeling framework (called "UW-VIC" therein) was assessed over the West Siberian Lowland over the period 1993-2004, relative to observations, several atmospheric inversions (including those of Bousquet et al. (2011)), and many other process-based models. While there was little agreement across these datasets in terms of interannual variability, th~~ose~~e process-based models (including UW-VIC) that employed soil physics formulations appropriate to high-latitudes and realistic relationships between CH_4 emissions and water table depth tended to be more similar to the inversions than those that did not. Our investigation of parameter uncertainty (Figures 9 and 10) revealed a substantial range in sensitivities and end-of-century CH_4 emissions, but made little difference to the shape of the trajectory over the next century or the spatial distribution of climate controls. Thus, we ~~we~~ believe our findings here are robust ~~against~~with respect to parameter uncertainty. However, investigation of the impacts of model uncertainty on climate controls on CH_4 emissions using other model formulations ~~may~~would be ~~warranted~~useful.

4.2 Sensitivity-Based Future Projections

Our sensitivity estimates provide a simplified description of wetland behavior; in effect, a linearization of our process-based model. Nevertheless, the similarity between our process-based and sensitivity-based projections suggests that our domain-averaged sensitivities capture most of the dependence of CH_4 emissions on climate conditions, as represented within our modeling framework. Our projected emissions are comparable to those of other process-based studies. Our estimate of a 24-32% increase in pan-Arct~~e~~ic CH4 emissions by mid-

century is comparable to the 25% increase estimated by Anisimov (2011). Over northern Eurasia, our estimate of end-of-century emissions is 21.5 $TgCH_4$ y^{-1}, similar to the estimate of 25.1±3.7 $TgCH_4$ y^{-1} by Zhu et al. (2011). The widespread warming and drying of wetlands and consequent reduced sensitivity of emissions to warming in our projections are consistent with similar findings in other studies (Koven et al., 2011; Riley et al., 2011; Ringeval et al., 2011; Lawrence et al., 2015).

Our characterization of the sensitivities of emissions to climate requires the assumption that, as a grid cell's climate changes, its future sensitivities will come to resemble those of cells with similar climate today; in essence attributing climate sensitivities completely to current climate state. Several studies have, however, found associations between vegetation and CH_4 emissions (Glagolev et al., 2011; Lupascu et al., 2012; Levy et al., 2012; Olefeldt et al., 2013). In particular, Olefeldt et al. (2013) found that emission rates from sedge-dominated wetlands are not only higher but also more sensitive to changes in both soil temperature and water table depth than are emission rates from non-sedge-dominated wetlands. On the other hand, dynamic vegetation models suggest that vegetation communities will migrate northward with future climate change (e.g., Kaplan and New, 2006; Alo and Wang, 2008), potentially bringing with them any characteristics (e.g., aerenchyma) that enhance CH_4 emissions. To the extent that vegetation communities can migrate in step with climate change, our sensitivity matrices would still be applicable. Nonetheless, this suggests an interesting avenue for future research.

4.3   Future Changes in the Dominant Controls

In our future projections, we found that much of the region will shift from T+ limitation (colder than optimal) to T- and P+ limitation (warmer and drier than optimal). This large-scale shift towards the warm and dry side of the "ridge" of maximum emissions implies that air temperature will play a smaller role in end-of-century emissions than at present, for two reasons: first, the positive response to an increase in temperature in the northern portion of the domain will be partially or completely cancelled by the negative response from the southern portion; and second, the response to precipitation will increase due to the widespread drier-than-optimal conditions. This suggests that, beyond the year 2100, emissions may level off or even decrease under further climate change, unless precipitation can increase sufficiently to compensate for the increases in air temperature. The larger future role of P in controlling pan-

1   arctic CH_4 emissions may lead to greater uncertainty in future projections beyond 2100, due

2   to the poorer performance and greater lack of agreement of global climate models in

3   projecting future precipitation than temperature (Hawkins and Sutton, 2011; IPCC, 2014).

4   There are additional reasons to think that T will play a reduced role in the future. There is

5   some indication that the metabolic impacts of higher temperatures have been overestimated

6   by most models, as most studies neglect acclimatization. Koven et al., (2011), for instance,

7   found that soil microbial communities essentially adapt to warmer soil temperatures and CH_4

8   emissions rates return to their previous levels. Koven et al. (2011) showed that

9   acclimatization could eliminate over 50% of the increase in emissions over the Pan-Arctic by

10   the end of the century that would otherwise occur. Under such conditions, the primary effects

11   of increased T would then be on drying out the wetlands through increased ET. In addition,

12   because our model did not simulate dynamic vegetation phenology, we did not account for

13   increased transpiration arising from CO_2 fertilization, which also would have a drying effect

14   on the wetlands (the wetland-climate-CH_4 feedback as discussed by Ringeval et al., 2011,

15   ~~and~~ Koven et al., 2011, and Stocker et al., 2013). Including these effects in the model on

16   which our sensitivities were based would likely reduce the sensitivity of future emissions to

17   further increases in T and perhaps even change the sign of the sensitivity to negative in some

18   water-limited locations. Thus, our estimates of the expansion of the water-limited zone and

19   the reduction of the role of T may be considered a lower bound.

5   Conclusions

21   We performed an historical simulation of wetland CH_4 emissions for the Pan-Arctic domain,

22   1948-2006. In addition, we performed five experiments that investigated the sensitivities of

23   CH_4 emissions to changing climate, and two future projections over the period 2007-2106,

24   one process-based and the other based on CH_4 emission sensitivities to T, P and CO_2. Our

25   main conclusions are:

26   (1) We estimate the annual CH_4 emissions from Pan-Arctic wetlands averaged over 1997-

27   2006 at 35.0±6.7 $TgCH_4$ y^{-1}. This is ~~on the slightly higher end, but still~~ within the range

28   of previous estimates, but somewhat toward the higher end.~~This is slightly higher than~~

29   ~~(but within the range of) previous estimates~~.

30   (2) Based on our model, c~~C~~limate change over the last ~half century has led to a substantial

31   (20%) increase in total emitted CH_4, with increases in air temperature (and associated

32   downward longwave radiation) being the dominant driver. Increases in temperature and

[CO$_2$] were responsible for over 84% of the inferred increase in emissions. Most of the remainder is attributable to changes in shortwave radiation (decreasing) and precipitation (increasing).

(3) The dominance of air temperature is corroborated by the predominance of temperature-limited wetlands throughout most of the domain, with water-limited wetlands primarily occupying only the southernmost portion of the domain (south of 60° N latitude).

(4) Both process-based and sensitivity-based projections agreed that wetland CH$_4$ emissions from Pan-Arctic wetlands will increase to ~~135~~138-~~142~~153% of present-day levels by the end of this century. Because this study did not account for potential acclimatization or the wetland-climate-ch4 feedback resulting from CO$_2$ fertilization, this projected increase may be <u>overestimated</u>~~50% too high~~.

(5) As future climate across the pan-Arctic becomes warmer, northern wetlands are likely to shift from the current temperature-dominated state toward a more precipitation-dominated state due to a lack of sufficient increase in precipitation to compensate for higher evapotranspiration, and resultant soil drying. The resulting sensitivity of CH$_4$ emissions to further warming may then level off or even become negative.

Author Contributions

All co-authors jointly conceived and designed this study. X. Chen performed all model simulations and data analysis. X. Chen prepared the manuscript with contributions from all co-authors.

References

Alo, C. A., and Wang, G.: Potential future changes of the terrestrial ecosystem based on climate projections by eight general circulation models, J. Geophys. Res.-Biogeo., 113(G1), G01004, doi: 10.1029/2007JG000528, 2008.

Anisimov, O.: Potential feedback of thawing permafrost to the global climate system through methane emission, Environmental Research Letters, 2, 045016, doi: 10.1088/1748-9326/2/4/045016, 2007.

Bartlett, K. B. and Harriss, R. C.: Review and assessment of methane emissions from wetlands, Chemosphere, 26, 261-320, doi: 10.1016/0045-6535(93)90427-7, 1993.

Bohn, T., Lettenmaier, D., Sathulur, K., Bowling, L., Podest, E., McDonald, K. and Friborg, T.: Methane emissions from western Siberian wetlands: heterogeneity and sensitivity to climate change, Environmental Research Letters, 2, 045015, doi: 10.1088/1748-9326/2/4/045015, 2007.

Bohn, T. J., Podest, E., Schroeder, R., Pinto, N., McDonald, K. C., Glagolev, M., Filippov, I., Maksyutov, S., Heimann, M., Chen, X., and Lettenmaier, D. P.: Modeling the large-scale effects of surface moisture heterogeneity on wetland carbon fluxes in the West Siberian Lowland, Biogeosciences, 10, 6559-6576, doi:10.5194/bg-10-6559-2013, 2013.

Bohn, T. J., Melton, J. R., Ito, A., Kleinen, T., Spahni, R., Stocker, B. D., Zhang, B., Zhu, X., Schroeder, R., Glagolev, M. V., Maksyutov, S., Brovkin, V., Chen, G., Denisov, S. N., Eliseev, A. V., Gallego-Sala, A., McDonald, K. C., Rawlins, M. A., Riley, W. J., Subin, Z. M., Tian, H., Zhuang, Q., and Kaplan, J. O.: WETCHIMP-WSL: intercomparison of wetland methane emissions models over West Siberia, Biogeosciences ~~Discuss.~~, 12, ~~1907-1973~~3321-3349, doi:10.5194/bg~~d~~-12-~~1907~~3321-2015, 2015.

Bovensmann, H., Burrows, J. P., Buchwitz, M., Frerick, J., Noël, S., Rozanov, V. V., Chance, K. V., and Goede, A. P. H.: SCIAMACHY: Mission objectives and measurement modes, J. Atmos. Sci., 56(2), 127-150, 1999.

Bousquet, P., Ringeval, B., Pison, I., Dlugokencky, E. J., Brunke, E.-G., Carouge, C., Chevallier, F., Fortems-Cheiney, A., Frankenberg, C., Hauglustaine, D. A., Krummel, P. B., Langenfelds, R. L., Ramonet, M., Schmidt, M., Steele, L. P., Szopa, S., Yver, C., Viovy, N.,

and Ciais, P.: Source attribution of the changes in atmospheric methane for 2006-2008, Atmos. Chem. Phys., 11, 3689-3700, doi: 10.5194/acp-11-3689-2011, 2011.

Brodzik, M. J. and Knowles, K. W.: "EASE-Grid: a versatile set of equal-area projections and grids", Discrete Global Grids, M. Goodchild (Ed.), Santa Barbara, California USA: National Center for Geographic Information & Analysis. http://www.ncgia.ucsb.edu/globalgrids-book/ease_grid/, 2002.

Brown J., Ferrians, O., Heginbottom, J. A., and Melnikov, E., Circum-Arctic Map of Permafrost and Ground Ice Conditions, Boulder, CO, USA: National Snow and Ice Data Center, [digital media], 2014.

Brutsaert, W., On a derivable formula for long-wave radiation from clear skies, Water Resour. Res., 11(5), 742-744, doi: 10.1029/WRR011i005p00742, 1975.

Cao, M., Marshall, S. and Gregson, K.: Global carbon exchange and methane emissions from natural wetlands: Application of a process-based model, Journal of Geophysical Research: Atmospheres (1984–2012), 101, 14399-14414, doi: 10.1029/96JD00219, 1996.

Chen, Y. and Prinn, R. G.: Estimation of atmospheric methane emissions between 1996 and 2001 using a three-dimensional global chemical transport model, Journal of Geophysical Research: Atmospheres (1984–2012), 111, D10307, doi: 10.1029/2005JD006058, 2006.

Christensen, T., Prentice, I., Kaplan, J., Haxeltine, A. and Sitch, S.: Methane flux from northern wetlands and tundra, Tellus B, 48, 652-661, 1996.

Christensen, T. R., Ekberg, A., Ström, L., Mastepanov, M., Panikov, N., Öquist, M., Svensson, B. H., Nykänen, H., Martikainen, P. J. and Oskarsson, H.: Factors controlling large scale variations in methane emissions from wetlands, Geophys. Res. Lett., 30(7), 1414, doi: 10.1029/2002GL016848, 2003.

Diffenbaugh, N. S. and Giorgi, F.: Climate change hotspots in the CMIP5 global climate model ensemble, Clim. Change, 114, 813-822, doi: 10.1007/s10584-012-0570-x, 2012.

Eliseev, A. V., Mokhov, I. I., Arzhanov, M. M., Demchenko, P. F., and Denisov, S. N.: Interaction of the methane cycle and processes in wetland ecosystems in a climate model of intermediate complexity, Izv. Atmos. Ocean. Phy., 44(2), 139-152, doi: 10.1134/S0001433808020011, 2008.

1　Fang, W. and Yihui, D.: Validation of Simulation on Surface Shortwave Radiation over East
2　Asia by Global Climate Models, Journal of Applied Meteorological Science, 19, 749-759,
3　doi: 10.3969/j.issn.1001-7313.2008.06.015, 2009.

4　Friborg, T., Soegaard, H., Christensen, T. R., and Panikov, N. S.: Siberian wetlands: Where a
5　sink is a source, Geophys. Res. Lett., 30(21), 2129, doi: 10.1029/2003GL017797, 2003.

6　Friedl, M. A., Sulla-Menashe, D., Tan, B., Schneider, A., Ramankutty, N., Sibley, A., and
7　Huang, X.: MODIS Collection 5 global land cover: algorithm refinements and
8　characterization of new datasets, Remote Sens. Environ., 114, 168-182, doi:
9　10.1016/j.rse.2009.08.016, 2010.

10　Fung, I., John, J., Lerner, J., Matthews, E., Prather, M., Steele, L. and Fraser, P.: Three-
11　dimensional model synthesis of the global methane cycle, Journal of Geophysical Research:
12　Atmospheres (1984–2012), 96, 13033-13065, doi: 10.1029/91JD01247, 1991.

13　Gedney, N., Cox, P. and Huntingford, C.: Climate feedback from wetland methane emissions,
14　Geophys. Res. Lett., 31, L20503, doi: 10.1029/2004GL020919, 2004.

15　Glagolev, M., Kleptsova, I., Filippov, I., Maksyutov, S. and Machida, T.: Regional methane
16　emission from West Siberia mire landscapes, Environmental Research Letters, 6, 045214, doi:
17　10.1088/1748-9326/6/4/045214, 2011.

18　Gurney, K., Law, R., Rayner, P. and Denning, A.: Transcom 3 experimental protocol,
19　Department of Atmospheric Science, Colorado State University USA, 2000.

20　Hawkins, E., and Sutton, R.: The potential to narrow uncertainty in projections of regional
21　precipitation change, Clim. Dyn., 37(1-2), 407-418, 2011.

22　Hein, R., Crutzen, P. J. and Heimann, M.: An inverse modeling approach to investigate the
23　global atmospheric methane cycle, Global Biogeochem. Cycles, 11, 43-76, doi:
24　10.1029/96GB03043, 1997.

25　Intergovernmental Panel on Climate Change (IPCC): Climate Change 1995: The Science of
26　Climate Change. Contribution of Working Group I to the Second Assessment Report of the
27　Intergovernmental Panel on Climate Change, [Houghton, J. T., Meira Filho, L. G., Callander,
28　B. A., Harris, N., Kattenberg, A., and Maskell, K. (eds.)]. Cambridge University Press,
29　Cambridge, United Kingdom and New York, NY, USA, 572 pp, 1996.

Intergovernmental Panel on Climate Change (IPCC): Climate Change 2013: The Physical Science Basis. Contribution of Working Group I to the Fifth Assessment Report of the Intergovernmental Panel on Climate Change, [Stocker, T.F., D. Qin, G.-K. Plattner, M. Tignor, S.K. Allen, J. Boschung, A. Nauels, Y. Xia, V. Bex and Midgley, P. M. (eds.)]. Cambridge University Press, Cambridge, United Kingdom and New York, NY, USA, 1535 pp, doi:10.1017/CBO9781107415324, 2013.

Kalnay, E., Kanamitsu, M., Kistler, R., Collins, W., Deaven, D., Gandin, L., Iredell, M., Saha, S., White, G., Woollen, J., Zhu, Y., Leetmaa, A., Reynolds, R., Chelliah, M., Ebisuzaki, W., Higgins, W., Janowiak, J., Mo, K. C., Ropelewski, C., Wang, J., Jenne, R., and Joseph, D.: The NCEP/NCAR 40-year reanalysis project, B. Am. Meteorol. Soc., 77, 437-471, doi: 10.1175/1520-0477/(1996)077<0477:TNYRP>2.0.CO;2, 1996.

Kaplan, J. O., and New, M.: Arctic climate change with a 2 degrees C global warming: Timing, climate patterns and vegetation change, Climatic Change, 79(3-4), 213-241, doi: 10.1007/s10584-006-9113-7, 2006.

Kim, H., Maksyutov, S., Glagolev, M., Machida, T., Patra, P., Sudo, K. and Inoue, G.: Evaluation of methane emissions from West Siberian wetlands based on inverse modeling, Environmental Research Letters, 6, 035201, doi: 10.1088/1748-9326/6/3/035201, 2011.

Lawrence, D. M., Koven, C. D., Swensen, S. C., Riley, W. J., and Slater, A. G.: Permafrost thaw and resulting soil moisture changes regulate projected high-latitude CO_2 and CH_4 emissions, Environ. Res. Lett., 10, 094011, doi: 10.1088/1748-9326/10/9/094011.

Lehner, B. and Döll, P.: Development and validation of a global database of lakes, reservoirs and wetlands, Journal of Hydrology, 296, 1-22, doi: 10.1073/pnas.1103910108, 2004.

Levy, P. E., Burden, A., Cooper, M. D., Dinsmore, K. J., Drewer, J., Evans, C., Fowler, D., Gaiawyn, J., Gray, A. and Jones, S. K.: Methane emissions from soils: synthesis and analysis of a large UK data set, Global Change Biol., 18, 1657-1669, doi: 10.1111/j.1365-2486.2011.02616.x, 2012.

Liang, X., Lettenmaier, D. P., Wood, E. F., and Burges, S. J.: A simple hydrologically based model of land surface water and energy fluxes for GSMs, J. Geophys. Res.-Atmos., 99(D7), 14415-14428, 1994.

Liu, Y., Zhuang, Q., Miralles, D., Pan, Z., Kicklighter, D., Zhu, Q., He, Y., Chen, J., Tchebakova, N., Sirin, A., Niyogi, D., and Melillo, J.: Evapotranspiration in Northern

Eurasia: Impact of forcing uncertainties on terrestrial ecosystem model estimates, J. Geophys. Res.-Atmos., 120, 10.1002/2014JD022531, 2015.

Lupascu, M., Wadham, J. L., Hornibrook, E. R. C., and Pancost, R. D.: Temperature sensitivity of methane production in the permafrost active layer at Stodalen, Sweden: a comparison with non-permafrost northern wetlands, Arct. Antarct. Alp. Res., 44(4), 469-482, doi: 10.1657/1938-4246-44.4.469, 2012.

Melton, J. R., Wania, R., Hodson, E., Poulter, B., Ringeval, B., Spahni, R., Bohn, T., Avis, C. A., Beerling, D. J., Chen, G., Eliseev, A. V., Denisov, S. N., Hopcroft, P. O., Lettenmaier, D. P., Riley, W. J., Singarayer, J. S., Subin, Z. M., Tian, H., Zurcher, S., Brovkin, V., van Bodegom, P. M., Kleinen, T., Yu, Z. C., and Kaplan, J. O.: Present state of global wetland extent and wetland methane modelling: Conclusions from a model intercomparison project (WETCHIMP), Biogeosciences, 10(2), 753-788, doi:10.5194/bg-10-753-2013, 2013.

Myneni, R. B., Hoffman, S., Knyazikhin, Y., Privette, J. L., Glassy, J., Tian, Y., Wang, Y., Song, X., Zhang, Y., Smith, G. R., Lotsch, A., Friedl, M., Morisette, J. T., Votava, P., Nemani, R. R., and Running, S. W.: Global products of vegetation leaf area and fraction absorbed PAR from year one of MODIS data, Remote Sens. Environ., 83, 214-231, doi: 10.1016/S0034-4257(02)00074-3, 2002.

Nemani, R. R., Keeling, C. D., Hashimoto, H., Jolly, W. M., Piper, S. C., Tucker, C. J., Myneni, R. B. and Running, S. W.: Climate-driven increases in global terrestrial net primary production from 1982 to 1999, Science, 300, 1560-1563, doi: 10.1126/science.1082750, 2003.

Olefeldt, D., Turetsky, M. R., Crill, P. M., and McGuire, A. D.: Environmental and physical controls on northern terrestrial methane emissions across permafrost zones, Global Change Biol., 19, 589-603, doi: 10.1111/gcb.12071, 2013.

Panikov, N. S., and Dedysh, S. N.: Cold season CH_4 and CO_2 emission from boreal peat bogs (West Siberia): Winter fluxes and thaw activation dynamics, Global Biogeochem. Cy., 14(4), 1071-1080, 2000.

Peregon, A., Maksyutov, S., Kosykh, N. P., Mironycheva-Tokareva, N. P.: Map-based inventory of wetland biomass and net primary production in western Siberia, J. Geophys. Res.-Biogeo., 113(G1), G01007, doi:10.1029/2007JG000441, 2008.

Pickett-Heaps, C. A., Jacob, D. J., Wecht, K. J., Kort, E. A., Wofsy, S. C., Diskin, G. S., Worthy, D. E. J., Kaplan, J. O., Bey, I., and Drevet, J.: Magnitude and seasonality of wetland

methane emissions from the Hudson Bay Lowlands (Canada), Atmos. Chem. Phys., 11, 3773-3779, doi: 10.5194/acp-11-3773-2011, 2011.

Riley, W., Subin, Z., Lawrence, D., Swenson, S., Torn, M., Meng, L., Mahowald, N. and Hess, P.: Barriers to predicting changes in global terrestrial methane fluxes: analyses using CLM4Me, a methane biogeochemistry model integrated in CESM, Biogeosciences, 8, 1925-1953, doi: 10.5194/bg-8-1925-2011, 2011.

Ringeval, B., Friedlingstein, P., Koven, C., Ciais, P., Noblet-Ducoudré, N. d., Decharme, B. and Cadule, P.: Climate-CH 4 feedback from wetlands and its interaction with the climate-CO 2 feedback, Biogeosciences, 8, 2137-2157, doi: 10.5194/bg-8-2137-2011, 2011.

Ringeval, B., de Noblet-Ducoudré, N., Ciais, P., Bousquet, P., Prigent, C., Papa, F. and Rossow, W. B.: An attempt to quantify the impact of changes in wetland extent on methane emissions on the seasonal and interannual time scales, Global Biogeochem. Cycles, 24, GB2003, doi: 10.1029/2008GB003354, 2010.

Running, S., Nemani, R. R., Heinsch, F. A., Zhao, M., Reeves, M., and Hashimoto, H.: A continuous satellite-derived measure of global terrestrial primary production, BioScience, 54(6), 547-560, doi: 10.1641/0006-3568(2004)054[0547:ACSMOG]2.0.CO;2, 2004.

Saarnio, S., Alm, J., Silvola, J., Lohila, A., Nykänen, H. and Martikainen, P. J.: Seasonal variation in CH4 emissions and production and oxidation potentials at microsites on an oligotrophic pine fen, Oecologia, 110, 414-422, doi: 10.1007/s004420050176, 1997.

Sabrekov, A., Runkle, B., Glagolev, M., Kleptsova, I. and Maksyutov, S.: Seasonal variability as a source of uncertainty in the West Siberian regional CH4 flux upscaling, Environmental Research Letters, 9, 045008, doi: 10.1088/1748-9326/9/4/045008, 2014.

Schaefer, K., Zhang, T., Bruhwiler, L., and Barrett, A. P.: Amount and timing of permafrost carbon release in response to climate warming, Tellus B, 63, 165-180, doi: 10.1111/j.1600-0889.2011.00527.x, 2011.

Schroeder, R., Rawlins, M. A., McDonald, K. C., Podest, E., Zimmermann, R., and Kueppers, M.: Satellite microwave remote sensing of North Eurasian inundation dynamics: development of coarse-resolution products and comparison with high-resolution synthetic aperture radar data, Environ. Res. Lett., 5(1), 015003, doi: 10.1088/1748-9326/5/1/015003, [available at http://wetlands.jpl.nasa.gov], 2010.

Schuldt, R., Brovkin, V., Kleinen, T. and Winderlich, J.: Modelling Holocene carbon accumulation and methane emissions of boreal wetlands–an Earth system model approach, Biogeosciences, 10, 1659-1674, doi: 10.5194/bg-10-1659-2013, 2013.

Seneviratne, S. I., Corti, T., Davin, E. L., Hirschi, M., Jaeger, E. B., Lehner, I., Orlowsky, B. and Teuling, A. J.: Investigating soil moisture–climate interactions in a changing climate: A review, Earth-Sci. Rev., 99, 125-161, doi: 10.1016/j.earscirev.2010.02.004, 2010.

Serreze, M. C., Walsh, J. E., Chapin, F. S., Osterkamp, T., Dyurgerov, M., Romanovsky, V., Oechel, W. C., Morison, J., Zhang, T., and Barry, R. G.: Observational evidence of recent change in the northern high-latitude environment, Climatic Change, 46(1-2), 159-207, doi: 10.1023/A:1005504031923, 2000.

Sheffield, J., Goteti, G. and Wood, E. F.: Development of a 50-year high-resolution global dataset of meteorological forcings for land surface modeling, J. Clim., 19, 3088-3111, doi: 10.1175/JCLI3790.1, 2006.

Sheng, Y., Smith, L. C., MacDonald, G. M., Kremenetski, K. V., Frey, K. E., Velichko, A. A., Lee, M., Beilman, D. W., and Dubinin, P.: A high-resolution GIS-based inventory of the west Siberian peat carbon pool, Global Biogeochem. Cy., 18(3), GB3004, doi: 10.1029/2003GB002190, 2004.

Slater, A. G., Bohn, T. J., McCreight, J. L., Serreze, M. C., and Lettenmaier, D. P.: A multimodel simulation of pan-Arctic hydrology, Journal of Geophysical Research, 112, G04S45, doi:10.1029/2006JG000303, 2007.

Spahni, R., Wania, R., Neef, L., Weele, M. v., Pison, I., Bousquet, P., Frankenberg, C., Foster, P., Joos, F. and Prentice, I.: Constraining global methane emissions and uptake by ecosystems, Biogeosciences, 8, 1643-1665, doi: 10.5194/bg-8-1643-2011, 2011.

Stocker, B. D., Roth, R., Joos, F., Spahni, R., Steinacher, M., Zaehle, S., Bouwman, L. and Prentice, I. C.: Multiple greenhouse-gas feedbacks from the land biosphere under future climate change scenarios, Nature Climate Change, 3, 666-672, 10.1038/nclimate1864, 2013.

Su, F., Adam, J. C., Trenberth, K. E. and Lettenmaier, D. P.: Evaluation of surface water fluxes of the pan-Arctic land region with a land surface model and ERA-40 reanalysis, Journal of Geophysical Research: Atmospheres (1984–2012), 111, D05110, doi: 10.1029/2005JD006387, 2006.

Tapley, B. D., Bettadpur, S., Ries, J. C., Thompson, P. F., and Watkins, M. M.: GRACE measurements of mass variability in the Earth system, Science, 305(5683), 503-505, doi: 10.1126/science.1099192, 2004.

Tarnocai, C., Canadell, J., Schuur, E., Kuhry, P., Mazhitova, G. and Zimov, S.: Soil organic carbon pools in the northern circumpolar permafrost region, Global Biogeochem. Cycles, 23, GB2023, doi: 10.1029/2008GB003327, 2009.

Teuling, A., Hirschi, M., Ohmura, A., Wild, M., Reichstein, M., Ciais, P., Buchmann, N., Ammann, C., Montagnani, L. and Richardson, A.: A regional perspective on trends in continental evaporation, Geophys. Res. Lett., 36, L02404, doi: 10.1029/2008GL036584, 2009.

Walter, B. P. and Heimann, M.: A process-based, climate-sensitive model to derive methane emissions from natural wetlands: Application to five wetland sites, sensitivity to model parameters, and climate, Global Biogeochem. Cycles, 14, 745-765, doi: 10.1029/1999GB001204, 2000.

Walter, B. P., Heimann, M., and Matthews, E.: Modeling modern methane emissions from natural wetlands: 1. Model description and results, J. Geophys. Res.-Atmos., 106(D24), 34189-34206, doi: 10.1029/2001JD900165, 2001.

Winderlich, J.: Setup of a CO2 and CH_4 measurement system in Central Siberia and modeling of its results. Technical Reports - Max-Planck-Institut für Biogeochemie 26, pp. 120, 2012.

Zhu, X., Zhuang, Q., Lu, X. and Song, L.: Spatial scale-dependent land–atmospheric methane exchanges in the northern high latitudes from 1993 to 2004, doi: 10.5194/bg-11-1693-2014, 2014.

Zhu, X., Zhuang, Q., Chen, M., Sirin, A., Melillo, J., Kicklighter, D., Sokolov, A. and Song, L.: Rising methane emissions in response to climate change in Northern Eurasia during the 21st century, Environmental Research Letters, 6, 045211, doi: 10.1088/1748-9326/6/4/045211, 2011.

Zhuang, Q., Melillo, J. M., Kicklighter, D. W., Prinn, R. G., McGuire, A. D., Steudler, P. A., Felzer, B. S. and Hu, S.: Methane fluxes between terrestrial ecosystems and the atmosphere at northern high latitudes during the past century: A retrospective analysis with a process-based biogeochemistry model, Global Biogeochem. Cycles, 18, GB3010, doi: 10.1029/2004GB002239, 2004.

1

1 **Tables**

2 Table 1. Parameter distributions used in the Walter and Heimann (2000) CH$_4$ model.

Type	r$_0$* [μmol L^{-1} h^{-1} (gC m^{-2} d^{-1})$^{-1}$]	xvmax [μmol L^{-1} h^{-1}]	Rkm [μmol L^{-1}]	rq$_{10}$ [-]	oxq$_{10}$ [-]
North	0.024	0.005	14.635	3.863	5.006
South	0.017	0.272	14.759	10.715	1.683

Region	Parameter	Units	Percentile		
			1st	50th	99th
North	r$_0$*	[μmol L^{-1} h^{-1} (gC m^{-2} d^{-1})$^{-1}$]	0.015	0.020	0.026
	xvmax	[μmol L^{-1} h^{-1}]	0.06	0.14	0.32
	rkm	[μmol L^{-1}]	4.2	11.0	13.9
	rq10	[-]	2.5	3.4	5.2
	oxq10	[-]	1.3	4.9	5.9
	tveg	[-]	6	11	15
South	r$_0$*	[μmol L^{-1} h^{-1} (gC m^{-2} d^{-1})$^{-1}$]	0.016	0.019	0.022
	xvmax	[μmol L^{-1} h^{-1}]	0.16	0.24	0.27
	rkm	[μmol L^{-1}]	13.0	16.1	17.1
	rq10	[-]	9.7	10.7	11.7
	oxq10	[-]	1.6	2.1	3.4
	tveg	[-]	7	12	15

3 Note: r$_0$* is the reference CH$_4$ production rate per unit annual average LAI (r$_0$* is related to
4 the original r$_0$ parameter from Walter and Heimann (2000) by r$_0$* = r$_0$/LAI$_{avg}$ as described in
5 Bohn et al. (2013)); xvmax is the maximum CH$_4$ oxidation rate; rRkm is the Michaelis
6 Menten constant for CH$_4$ oxidation; rq$_{10}$ is the Q$_{10}$ value for the CH$_4$ production rate; oxq$_{10}$ is

1 the Q_{10} value for the CH_4 oxidation rate; and tveg is a dimensionless integer value ranging

2 from 0 to 15 that indicates the strength of plant-aided transport.

3

4 Table 2.   Trends in spatial average climate factors, 1960-2006.

Factor	Trend
Mean annual air temperature (T)	0.0322 K y^{-1}
Annual precipitation (P)	0.5183 mm y^{-1}
Mean annual [CO_2]	1.4009 ppm y^{-1}
Mean annual shortwave radiation (SW)	-0.0385 W m^{-2} y^{-1}
Mean annual longwave radiation (LW)	0.0670 W m^{-2} y^{-1}

5

6 Table 3.   Estimates of total CH_4 emissions over the study domain.

Method	Estimate (TgCH_4 y^{-1})	Area	Reference	Period
VIC + Walter CH_4	35.0±6.7	Pan-Arctic wetlands	(This study)	1997-2006
VIC+TEM	38.1-55.4	Pan-Arctic area	Zhu et al. (2014)	1993-2004
MATCH (inversion)	34±13	N. hemisphere high latitude wetlands	Chen and Prinn, (2006)	1996-2001
Walter CH_4 model	56	Wetlands north of 45˚N	Walter et al. (2001)	1982-1993
Inversion	48	Wetlands north of 45˚N	Hein et al. (1997)	1983-1989
process-based model	20±13	Northern wetlands and tundra	Christensen et al. (1996)	1990s
WMEM	23.3	Wetlands north of	Cao et al.	-

		40˚N	(1996)	
(literature review)	35	N. hemisphere wetlands	IPCC (1996)	1980s – 1990s
(literature review)	38	Wetlands north of 45˚N	Bartlett and Harris (1993)	1980s

1

2 Table 4. Trends in CH_4 emissions from historical and control simulations, 1960-2006. All
3 values are in units of (Tg CH_4 y^{-1}).

Simulation	Trend	95% confidence bound	Driver Impact (historical trend - control trend)
R01 (historical)	0.158	(0.107, 0.207)	-
R02 (TLW control)	0.054	(0.006, 0.103)	0.104
R03 (CO2 control)	0.128	(0.079, 0.176)	0.030
R04 (TLWP control)	0.043	(-0.007, 0.093)	0.115
R05 (P control)	0.143	(0.093, 0.194)	0.015
R06 (SW control)	0.154	(0.104, 0.204)	0.004

4

5 Table 5. Spatial correlation coefficients between sensitivities and environmental factors.

Sensitivity of Annual CH_4 (g CH_4 m^{-2} y^{-1}) to:	Environmental Factor							
	JJA T^a (K)	JJA P^b	JJA $F_{inund}{}^c$	AM SWE^d (mm)	JJA LAI^e	ALD^f (m)	Annual NPP^g (g C m^{-2} y^{-1})	JJA $Tsoil^h$ (K)
JJA T(K)	0.1928	0.1827	0.0438	0.2990	0.1735	0.1813	0.2658	0.1682
|JJA P| (mm)*	0.2231	0.0309	-0.1068	-0.0530	0.1570	0.0797	0.1013	0.0462
[CO2] (ppm)	0.3856	0.3209	0.0887	0.2951	0.3364	0.3096	0.4541	0.3064

6 [a]JJA T = June-July-August average air temperature; [b]JJA P = June-July-August total
7 precipitation; [c]JJA F_{inund} = June-July-August inundated area fraction; [d]AM SWE = April-May

1 average snow water equivalent; [e]JJA LAI = June-July-August average leaf area index; [f]ALD

2 = maximum annual active layer depth; [g]Annual NPP = annual net primary productivity; [h]JJA

3 Tsoil = June-July-August average temperature in the top 10 cm of the soil column.

4 *Extreme values of sensitivity (> 0.005 g CH_4 m^{-2} y^{-1} per mm change in JJA P) were ignored;

5 these occurred at 164 cells, out of 2049 cells containing wetlands.

1 **Figures**
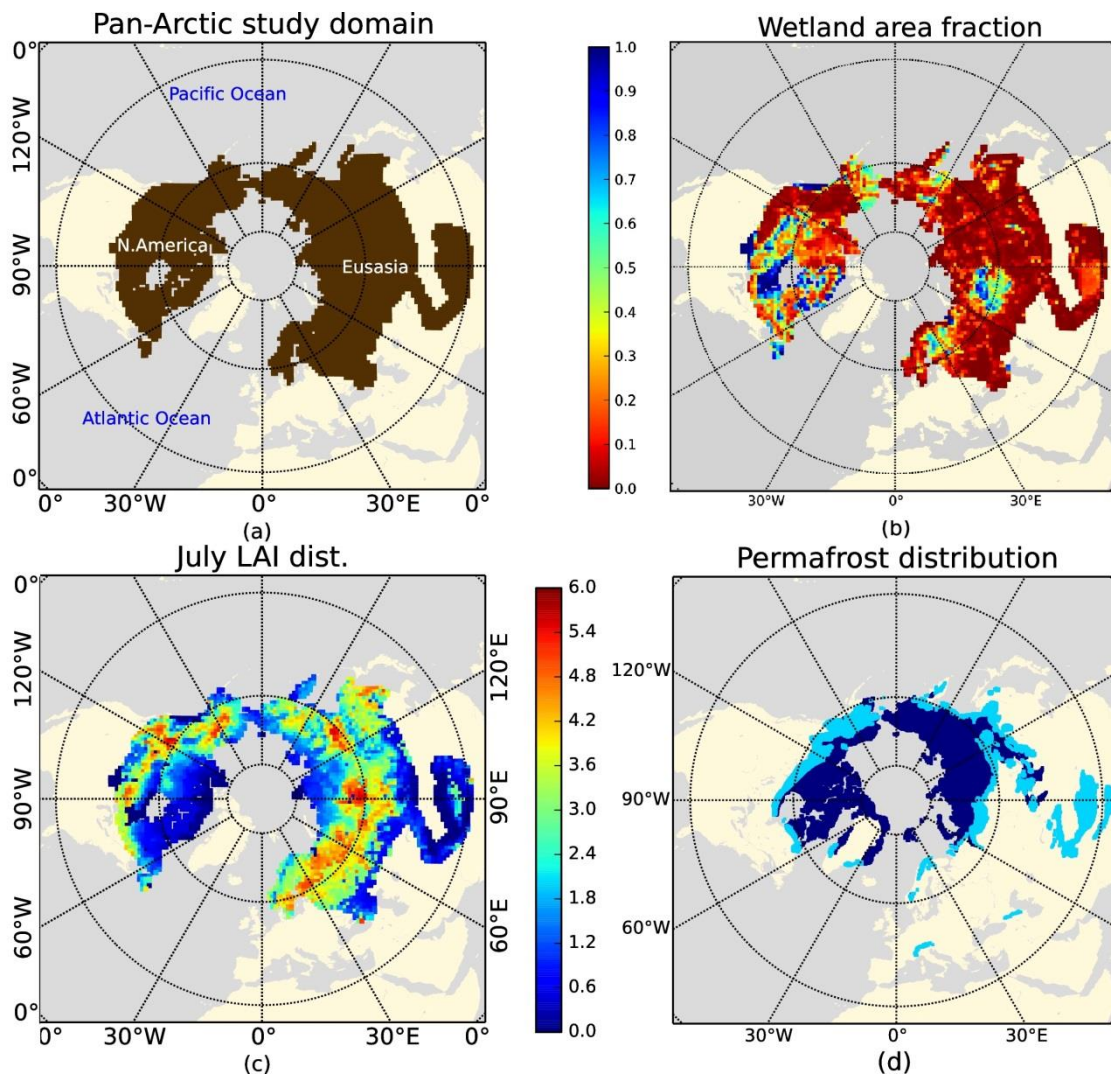
Figure 1. Relevant characteristics of study domain: (a) spatial extent of the domain; (b) lake/wetland area fractions (taken from Lehner and Döll, 2004, and Tarnocai et al., 2009; see text for details); (c) July LAI (taken from Myneni et al., 2002); (d) permafrost distribution (taken from Brown et al., 2014).

SWAMPS inundation fraction (a)

VIC inundation fraction (b)

CAMPGIC permafrost distribution (c)

VIC ALD (m) (d)

MODIS NPP, 2001-2006 (e)

VIC NPP, 2001-2006 (f)

VIC vs. MODIS NPP (g)

39

1
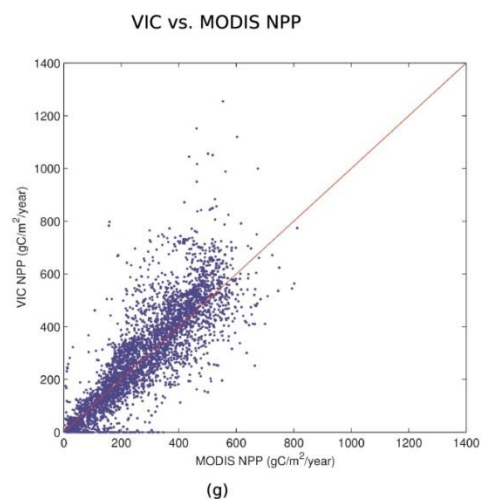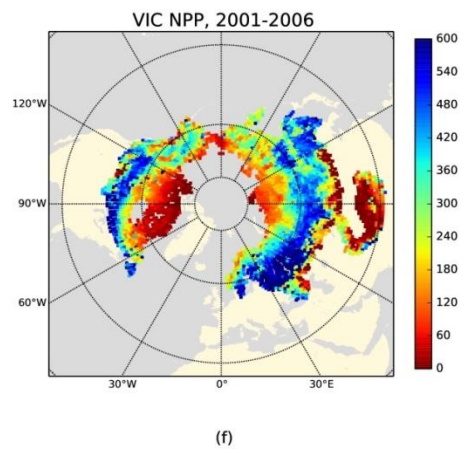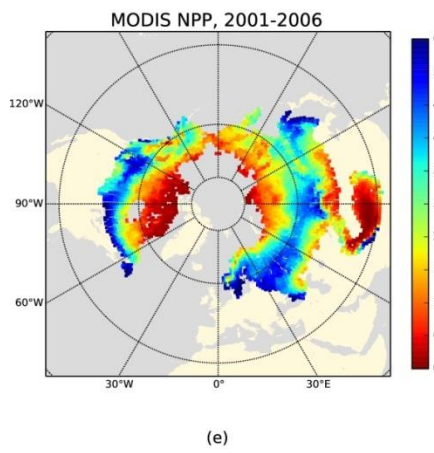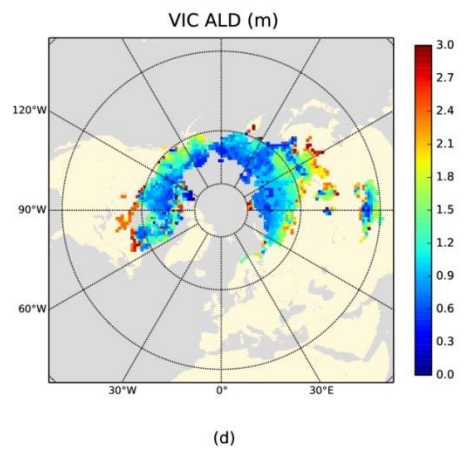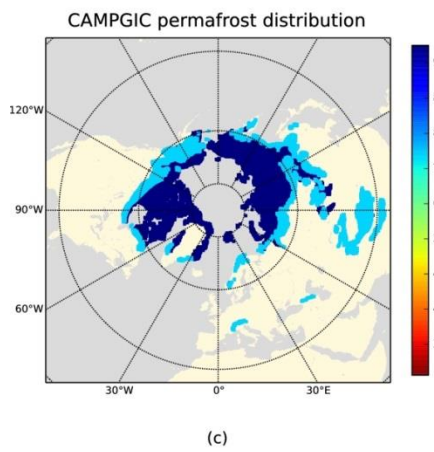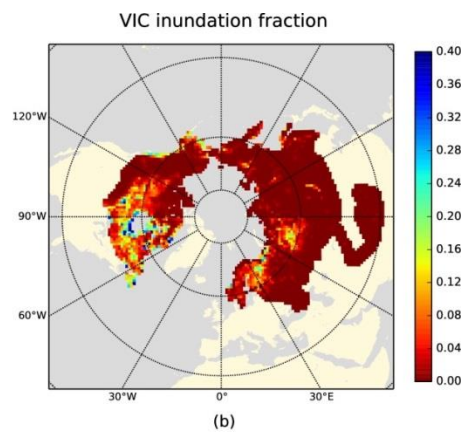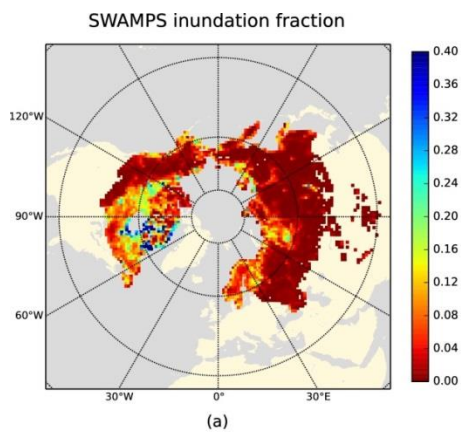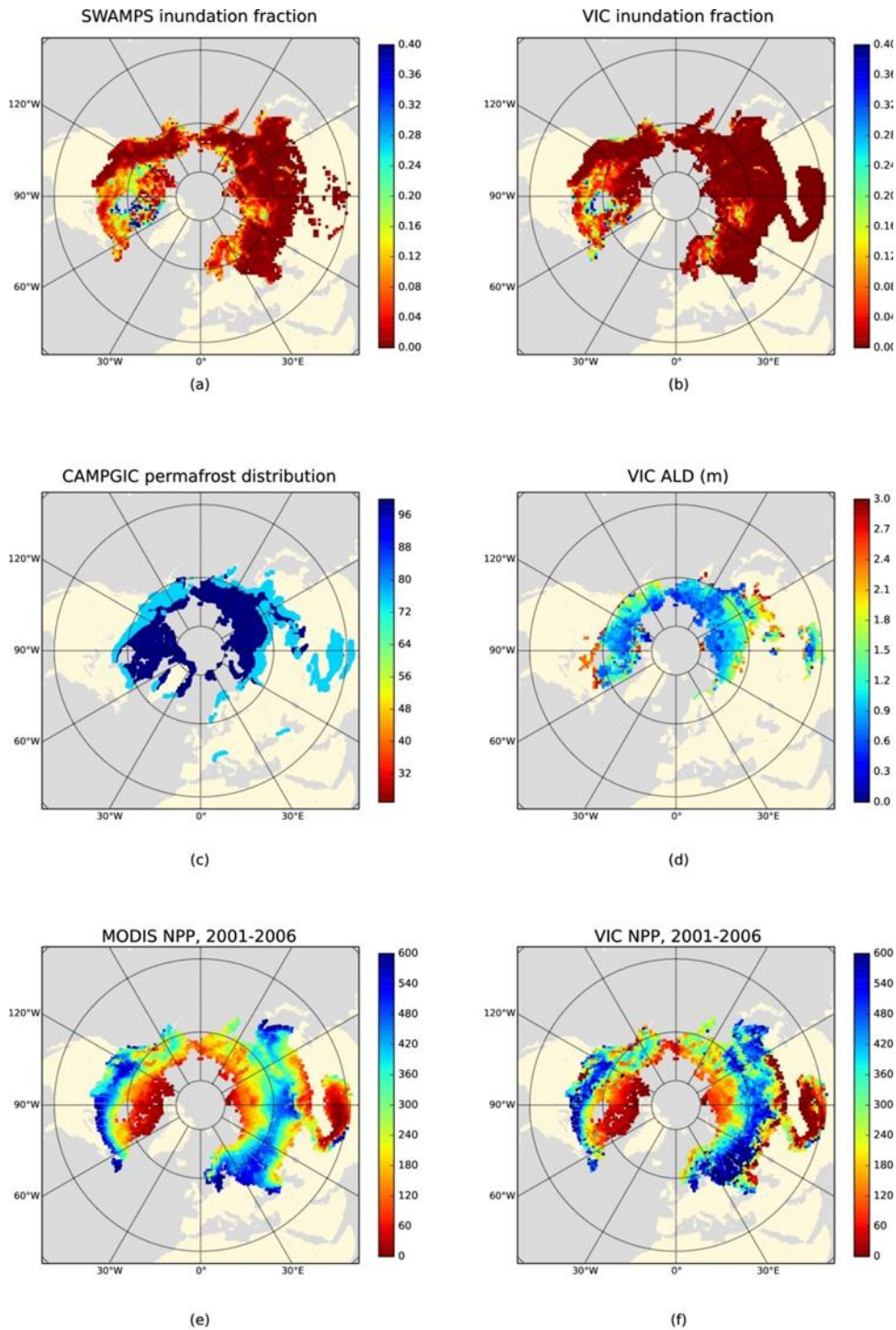
Figure 2. Observed and simulated factors relevant to wetland methane emissions over the study domain: (a) observed June-July-August average (JJA) inundated area fraction over 2002-2010 from SWAMPS (Schroeder et al., 2010); (b) simulated JJA inundated area fraction over 1948-2006; (c) observed permafrost distribution from CAMPGIC (Brown et al., 2014) (dark blue = continuous permafrost, light blue = discontinuous permafrost); (d) simulated maximum active layer depth (ALD) over 1948-2006; (e) observed JJA net primary

40

1 productivity (NPP) over 2002-2010 (Running et al., 2004); (f) simulated JJA LAI over 1948-

2 2006~~; (g) simulated JJA NPP vs observed JJA NPP~~.

3

4

Average annual CH$_4$ emission (gCH$_4$/m^2 /year)
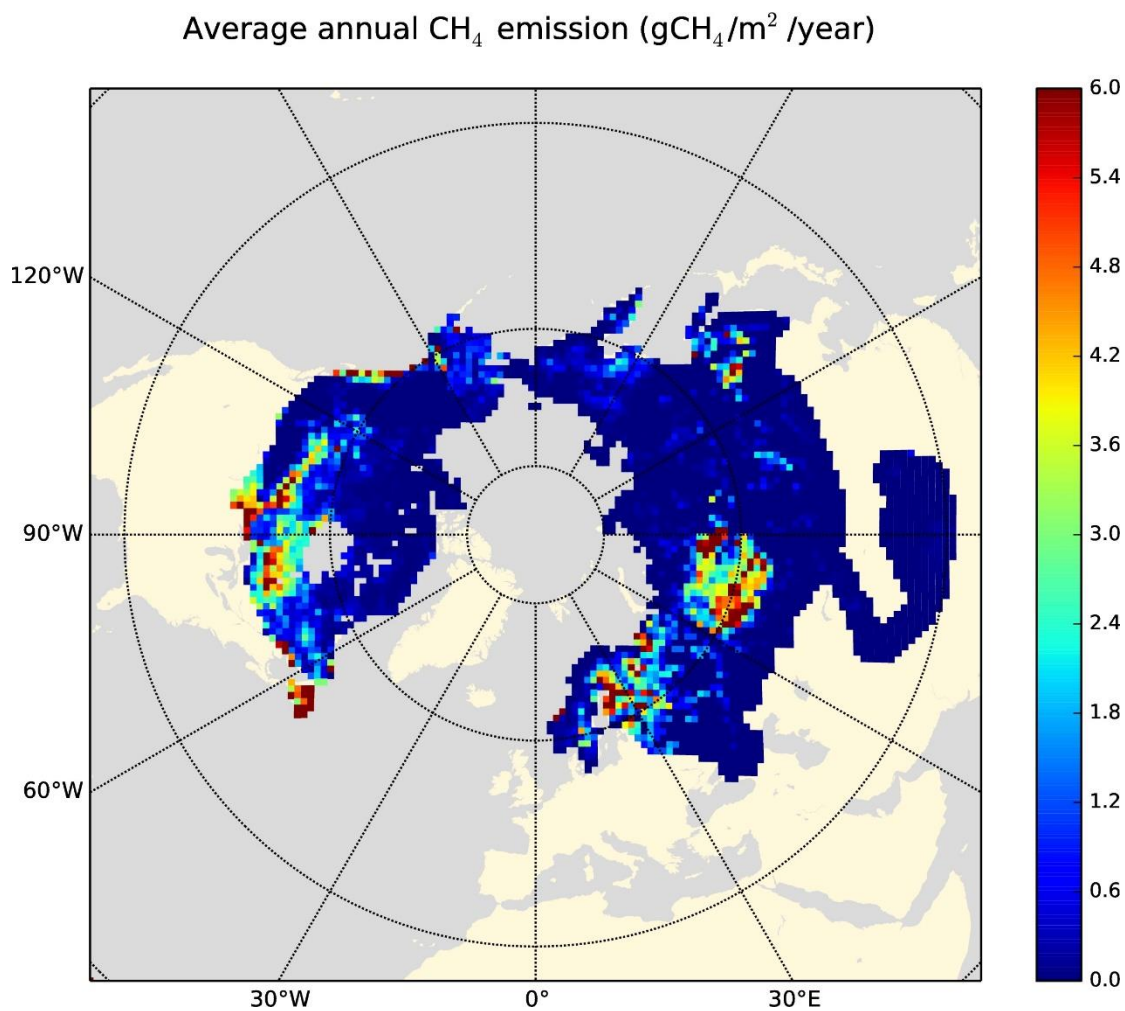
6 Figure 3. Average annual CH$_4$ emissions over the study domain, 1960-2006.

7

1   (a)   (b)
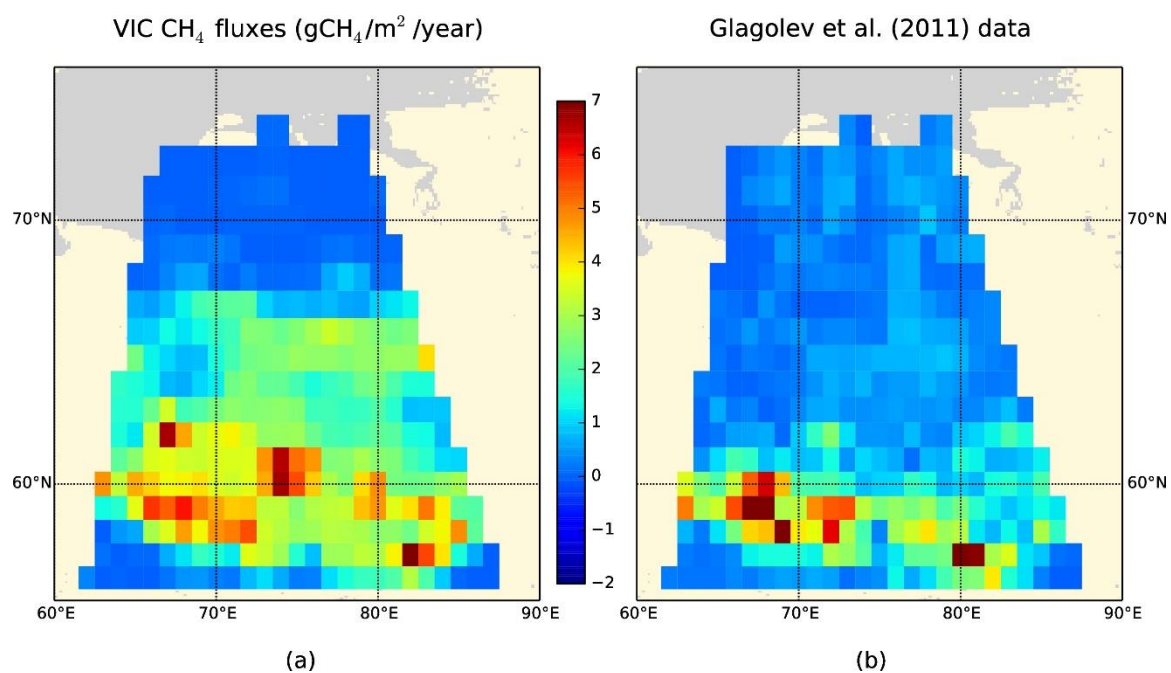
2   Figure 4.   Comparison of simulated CH_4 emission rate and field campaign based data over

3   WSL. (a) VIC simulated fluxes; (b) field campaign data based fluxes data from Glagolev et

4   al. (2011).

5
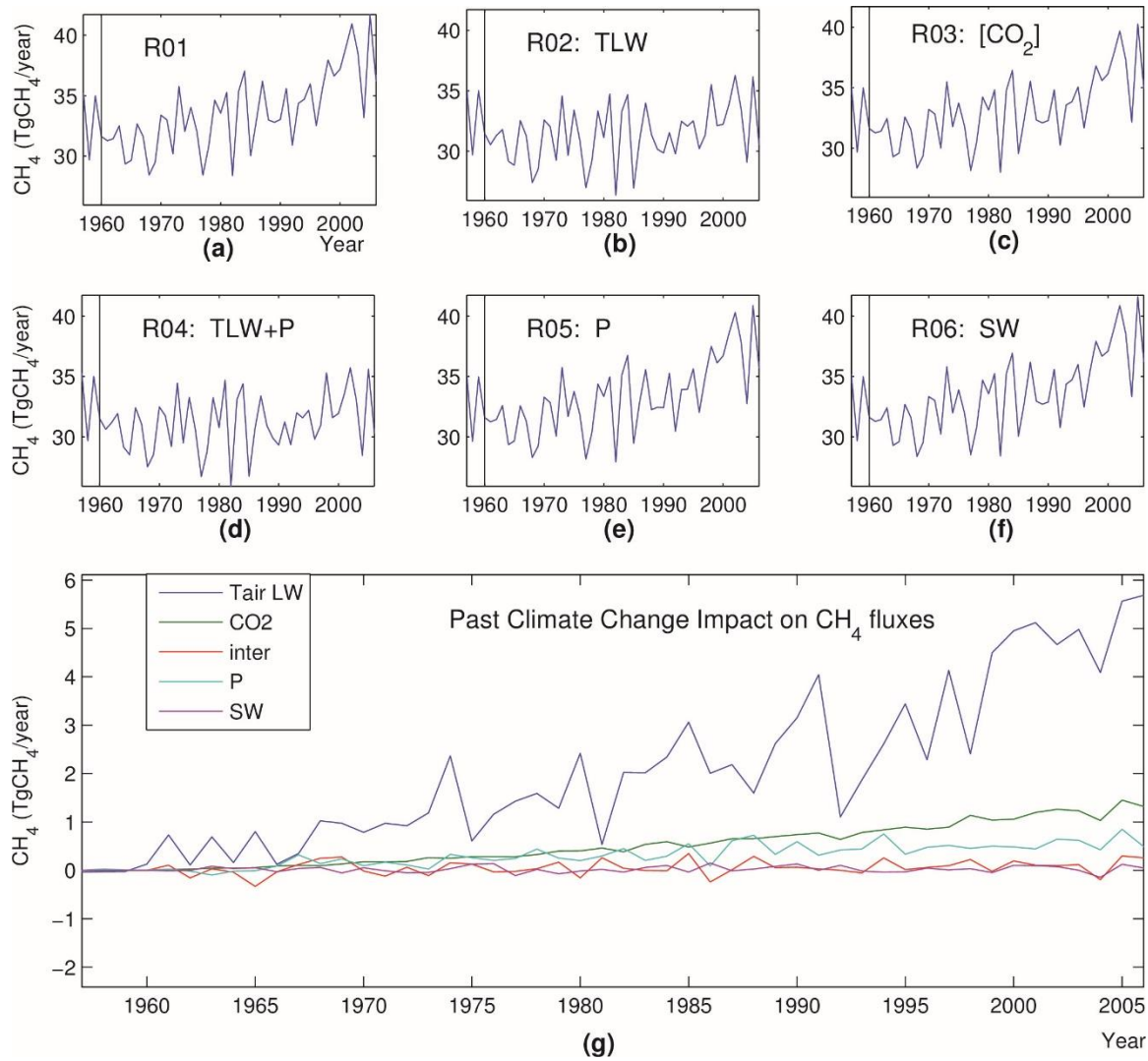
Figure 5. Timeseries of domain-averaged annual methane fluxes from (a) the historical simulation; (b-f) the five climate control runs, in each of which one climate driver was detrended starting in 1960; (g) differences between historical simulation in (a) and the control runs (b-f). "TLW" and "Tair LW" denote detrending of air temperature and associated downward longwave radiation; "CO_2" denotes detrending of atmospheric CO_2 concentrations; "TLW+P" denotes detrending of both air temperature (and associated longwave radiation) and precipitation; "P" denotes detrending of precipitation; "SW" denotes detrending of downward shortwave radiation; and "inter" denotes the difference between "TLW" and "TLW+P".

43
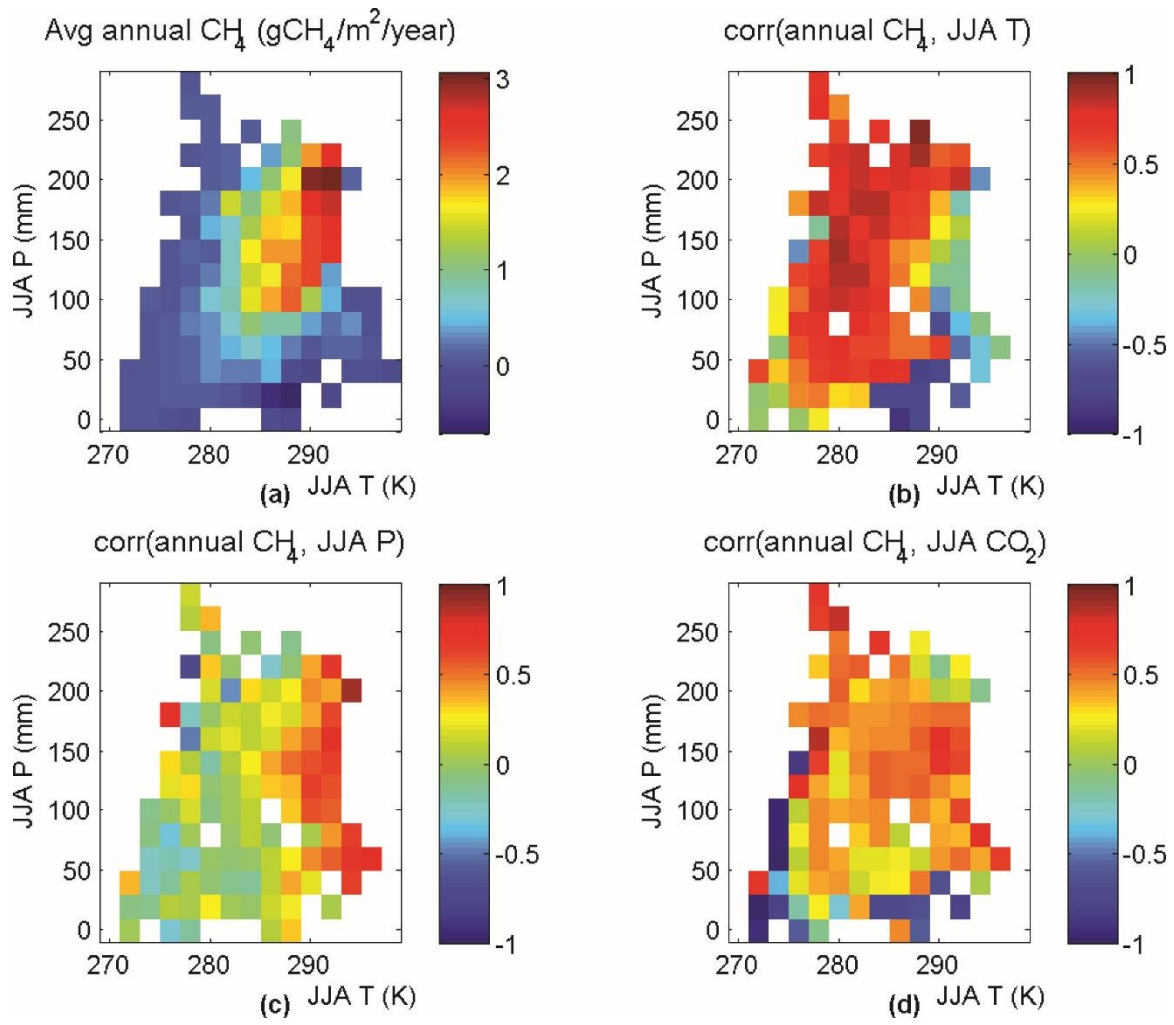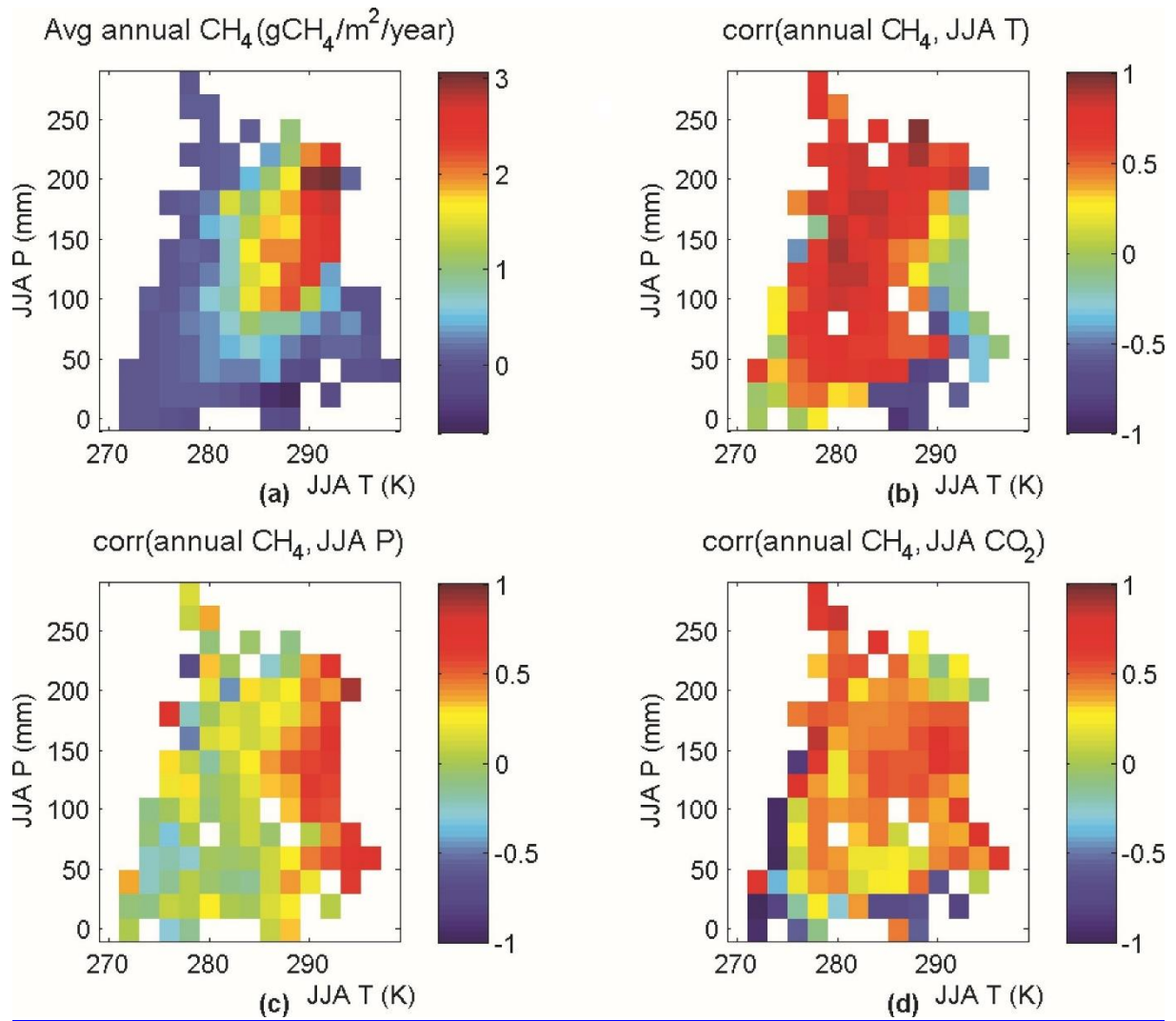
Figure 6. (a) the 1960-2006 average annual CH_4 emission over JJA (June-July-August) T and JJA P space; (b)-(d) correlation between 1960-2006 annual CH_4 emission and JJA drivers in the same T-P space.

Historical CH_4 emissions and JJA T, JJA P
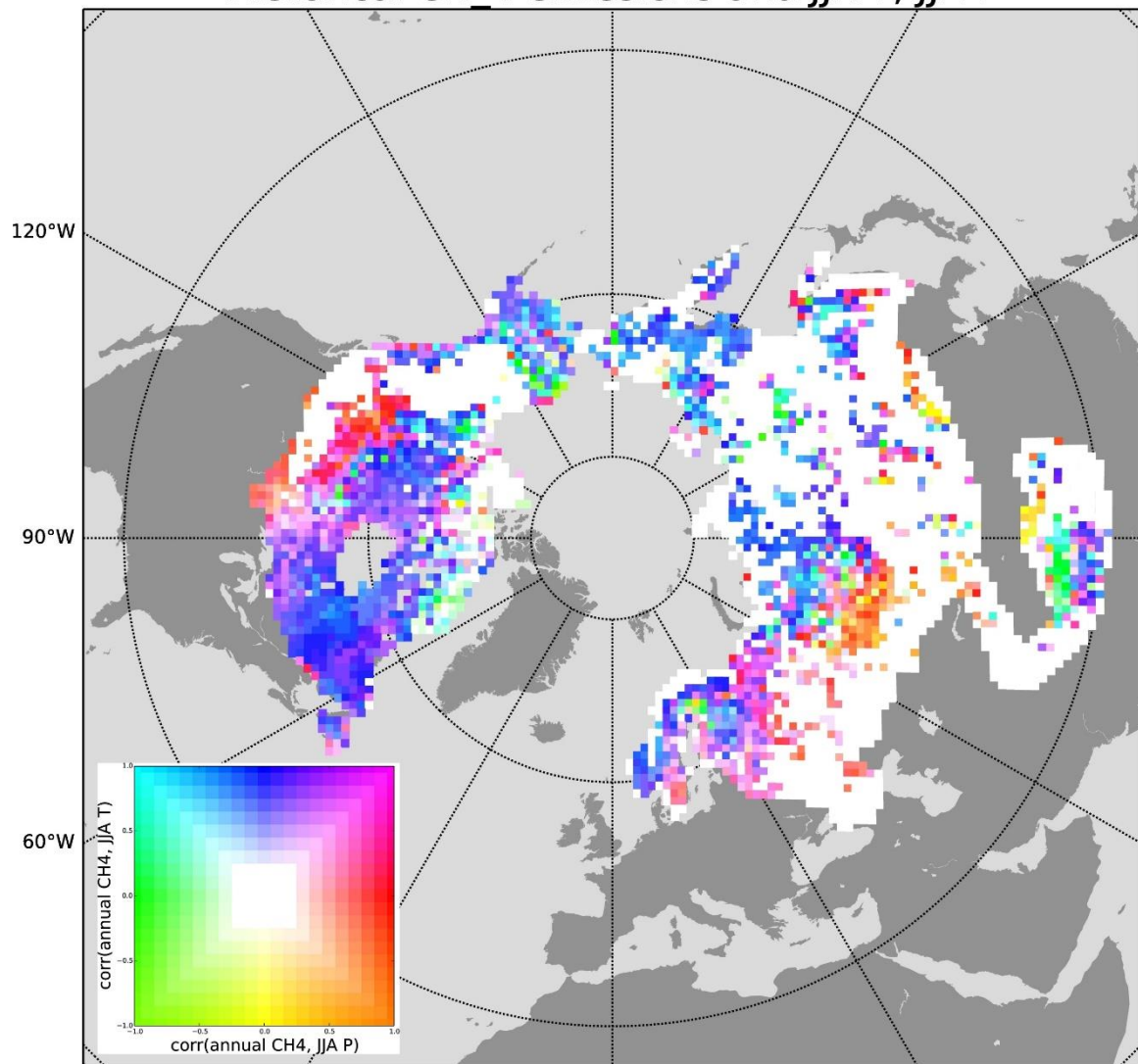
Historical climate (JJA T, JJA P) limit on CH4 emissions
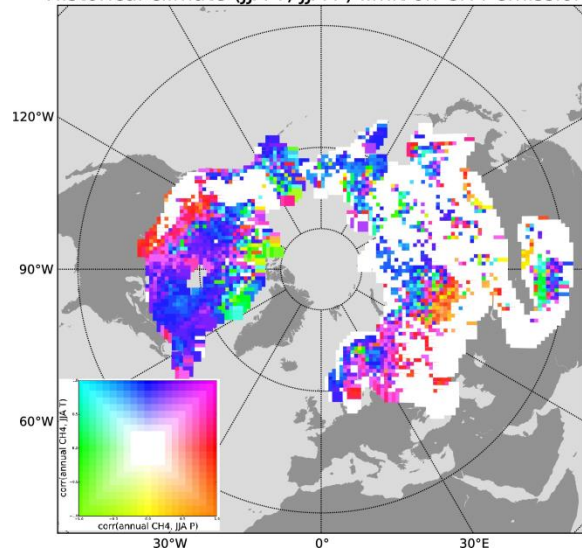
Range of uncertainties in the historical climate limit
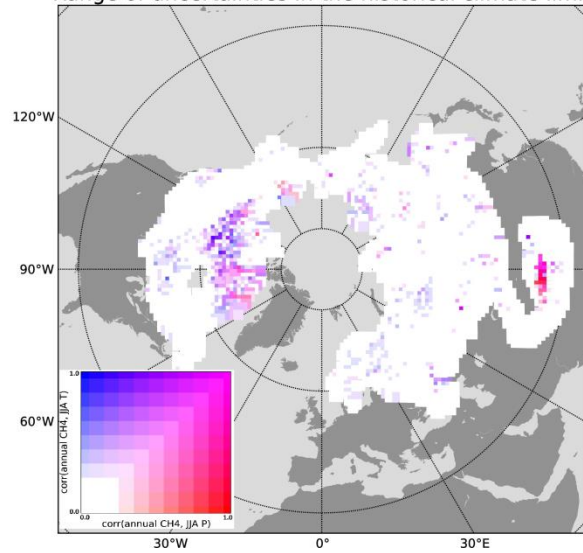
1   Figure 7. Spatial distributions of ensemble median (left) and range at 95% confidence level

2   (right) of correlations between annual CH$_4$ emissions and JJA T and ~~JJA~~ P.

3

(a)   (b)

4   (c)
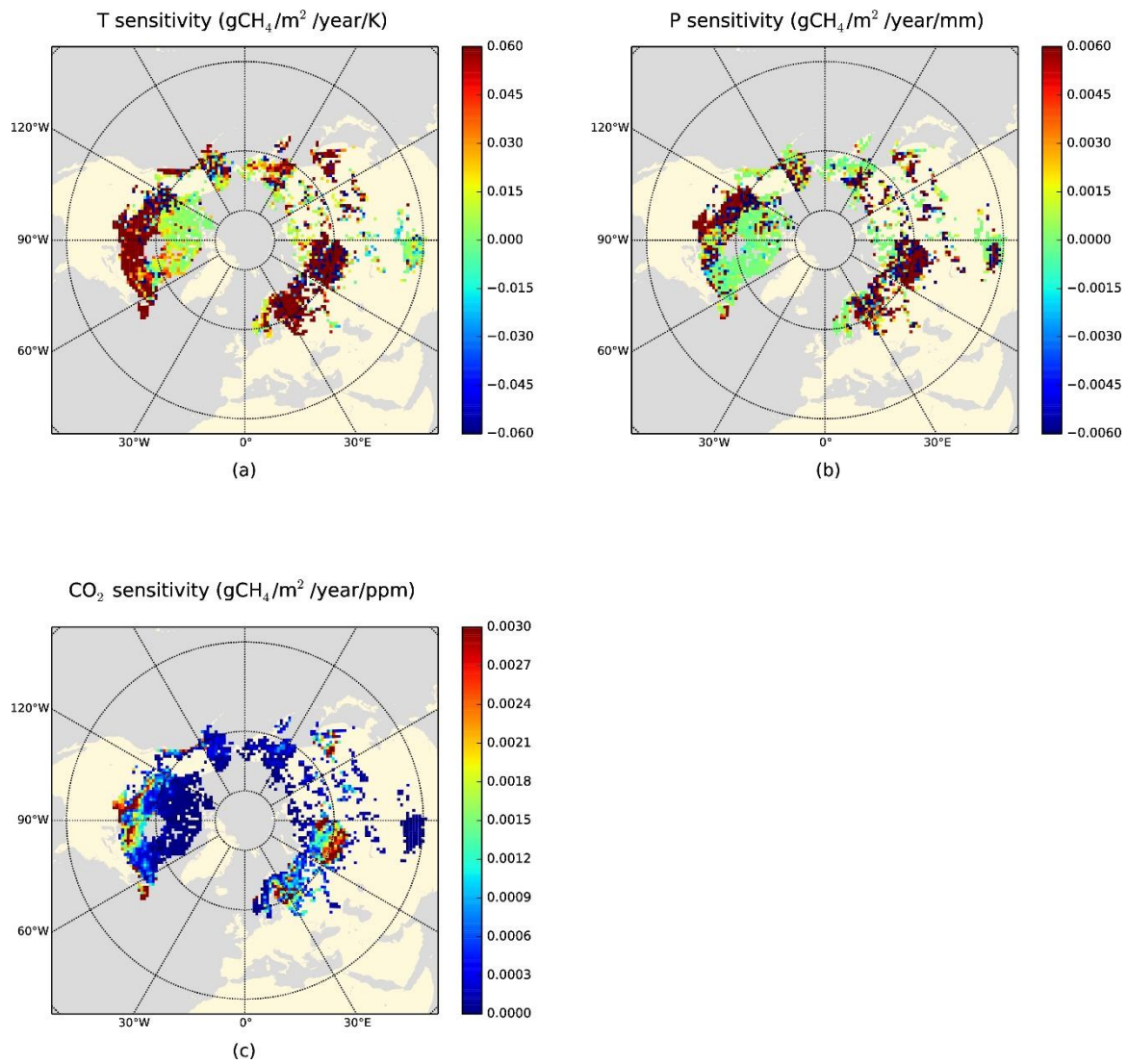
5   Figure 8. Spatial distributions of sensitivities of CH$_4$ to climate drivers. (a) sensitivity to air

6   temperature; (b) sensitivity to precipitation; (c) sensitivity to [CO$_2$].
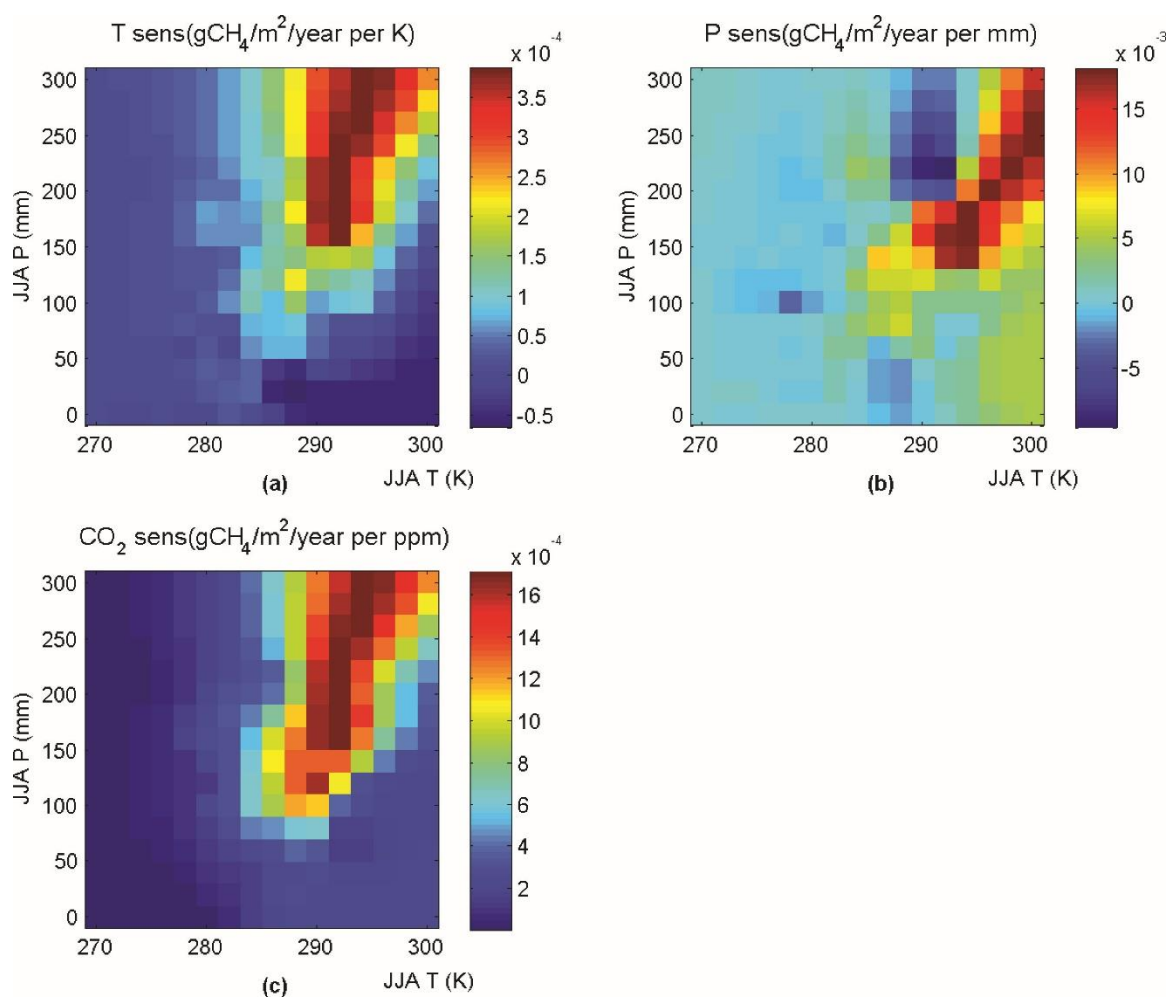
1
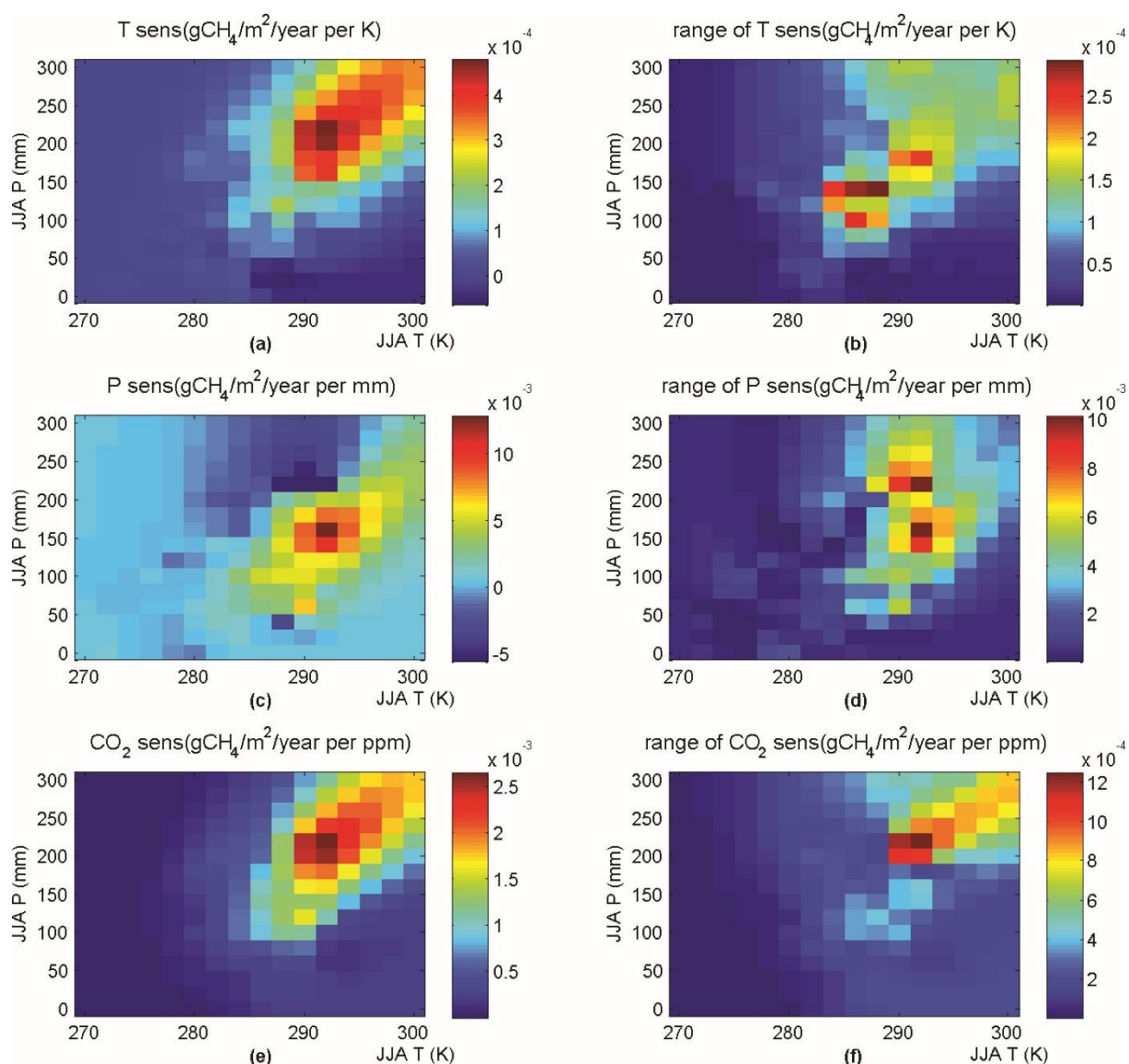
Figure 9. The 1960-2006 average T, P and CO_2 sensitivities of CH_4 emissions in JJA T and JJA P space using the median methane model parameter set (panels a, c, and e, respectively) and their ranges at the 95% confidence level across randomly-sampled methane model parameter sets (panels b, d, and f, respectively). Panels (a), (c) and (e) are the mean values of sensitivities, panels (b), (d) and (f) are the range of uncertainties, which is the maximum sensitivities minus the minimum value in each box.

Figure 10. Historical and projected annual methane emissions and climate drivers over the pan-Arctic, 2007-2106. (a) Sensitivity- and process-based projections (blue and black,

respectively) of methane emissions from northern wetlands during 2007-2106, with historical simulation (red) 1948-2006. ~~The~~Parameter-based uncertainties in the sensitivity-based projection ~~due to the uncertainties in the methane parameters~~ are ~~also~~ plotted as the yellow ~~(50% confidence bound)~~ and green envelopes (50% and 95~~8~~% confidence bounds, respectively); (b)-(d) climate conditions for projections. ~~Windows~~ The end-of-century window for time slice analy~~sis~~ (2096-2105) is denoted with vertical solid and dashed lines in panel (a)~~es are labeled: window 1 is 2026-2035, window 2 is 2056-2065, and window 3 is 2099-2105~~.

CH$_4$ 2026-2035 avg (gCH$_4$/m^2 /year) CH$_4$ 2056-2065 avg (gCH$_4$/m^2 /year) CH$_4$ 2096-2105 avg (gCH$_4$/m^2 /year)

(a) (b) (c)

diff from 2006 (gCH$_4$/m^2 /year) diff from 2006 (gCH$_4$/m^2 /year) diff from 2006 (gCH$_4$/m^2 /year)

(d) (e) (f)
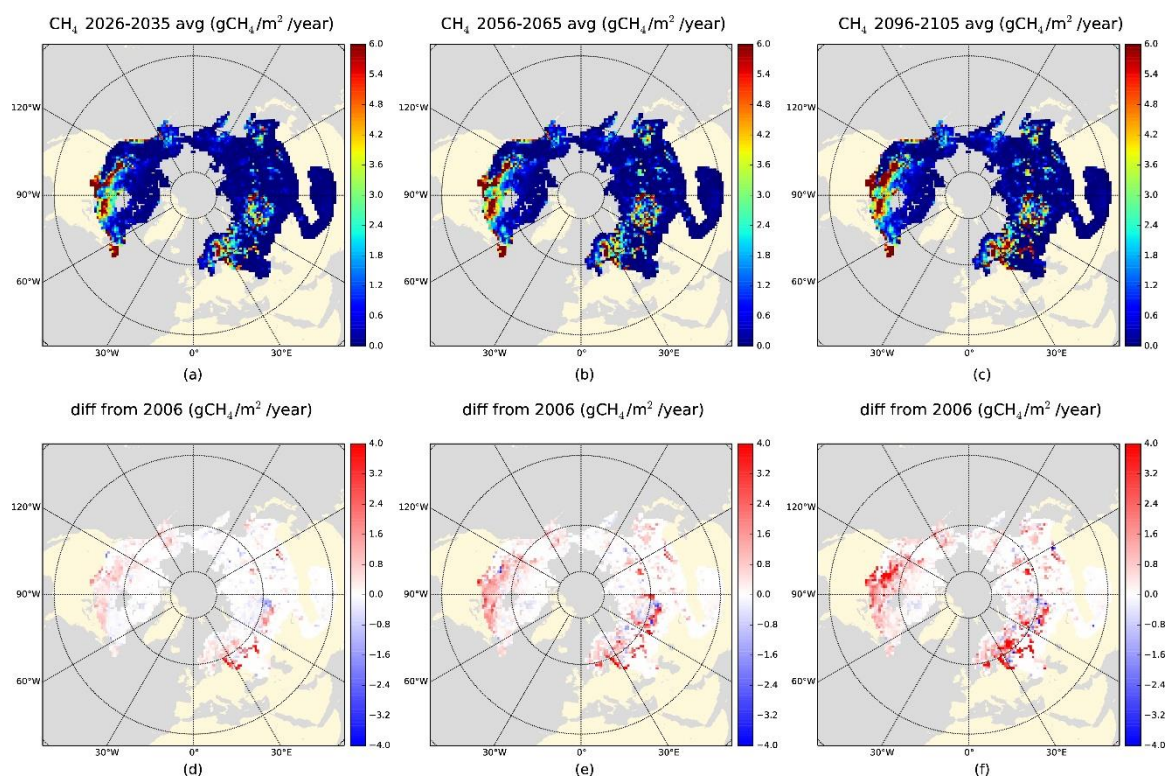
1

median of 2096-2105 avg CH₄ (gCH₄/m²/year)
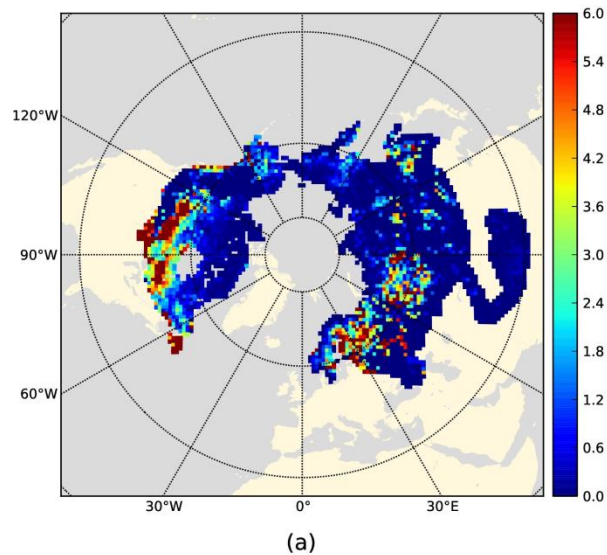
range of 2096-2105 avg CH₄ (gCH₄/m²/year)
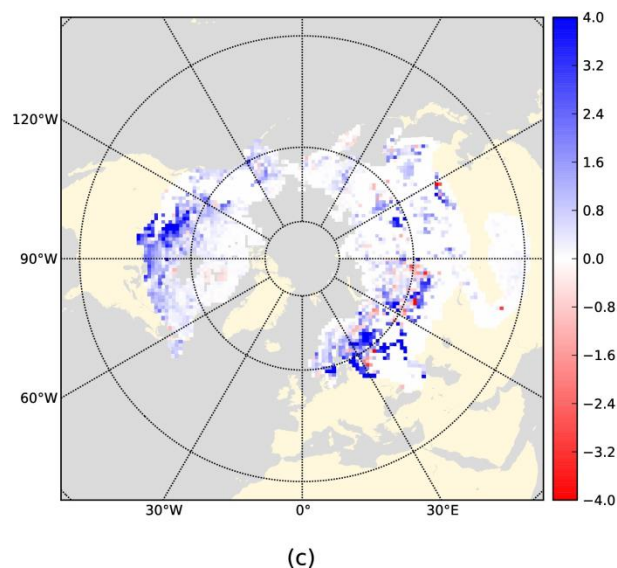
(a)

(b)
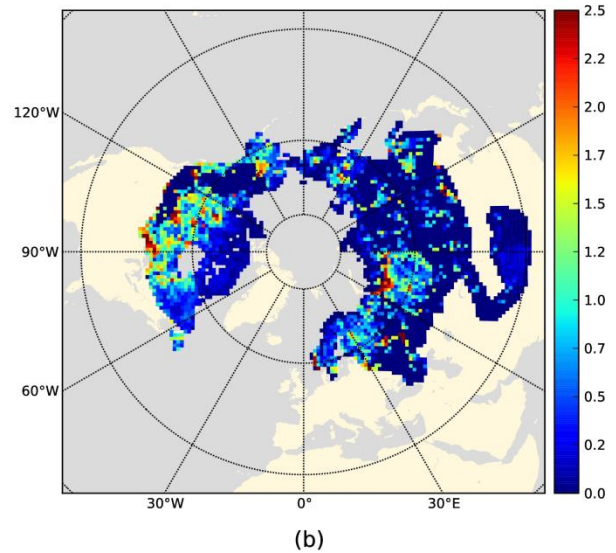
difference from 2006 (gCH₄/m²/year)

(c)

Figure 11. ~~Sensitivity-based projection~~Ensemble median (a) and range (b) of average annual end-of-century (2096-2105) ~~methane~~ CH₄ emissions ~~under future climate change, for the periods 2026-2035, 2056-2065, and 2096-2105~~for the sensitivity-based projection, and ~~their~~ difference~~s from~~ between the median and the annual emissions of year 2006 (c).
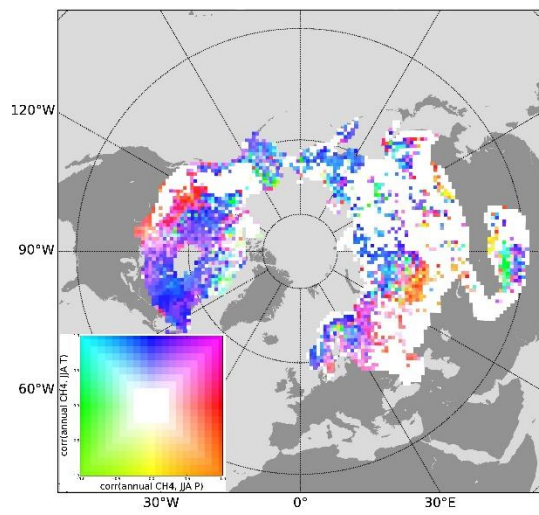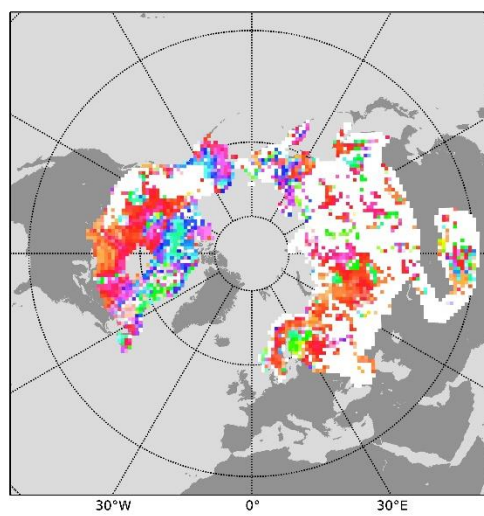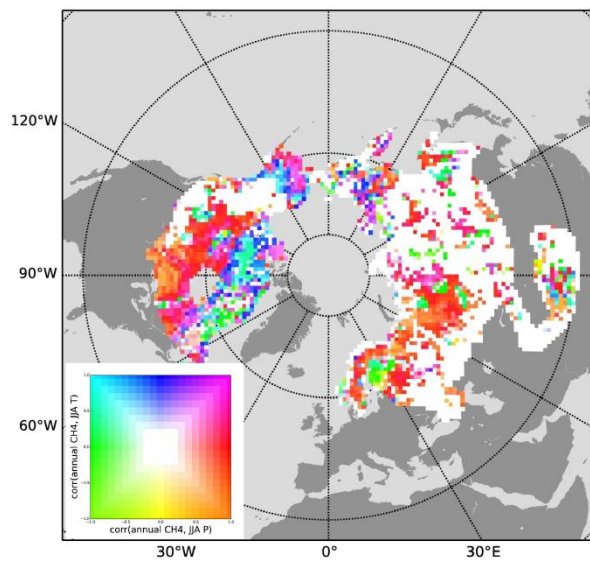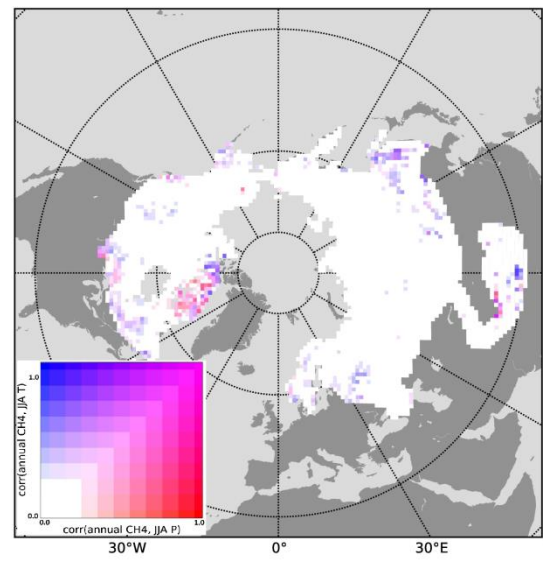
(a)
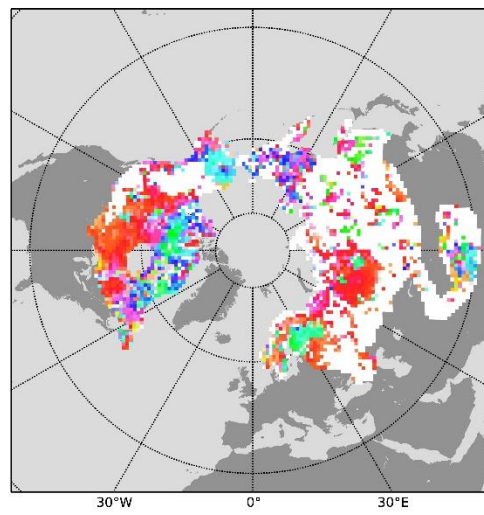
(b)
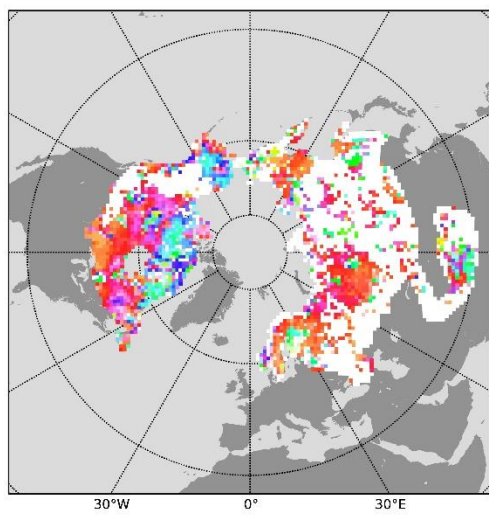
Median of corr(annual CH4, JJA driver), 2081-2100

Range of corr(annual CH4, JJA driver), 2081-2100

(a)

(b)

54

Figure 12. Spatial distributions ~~of~~ of ensemble median (left) and range at 95% confidence level (right) of correlations between annual CH$_4$ emissions and JJA T and P, ~~from (a) the historical simulation, 1960-2006; and (b) 2021-2040, (c) 2051-2070, and (d)~~for the period 2081-2100 of the ~~future~~ sensitivity-based projection.
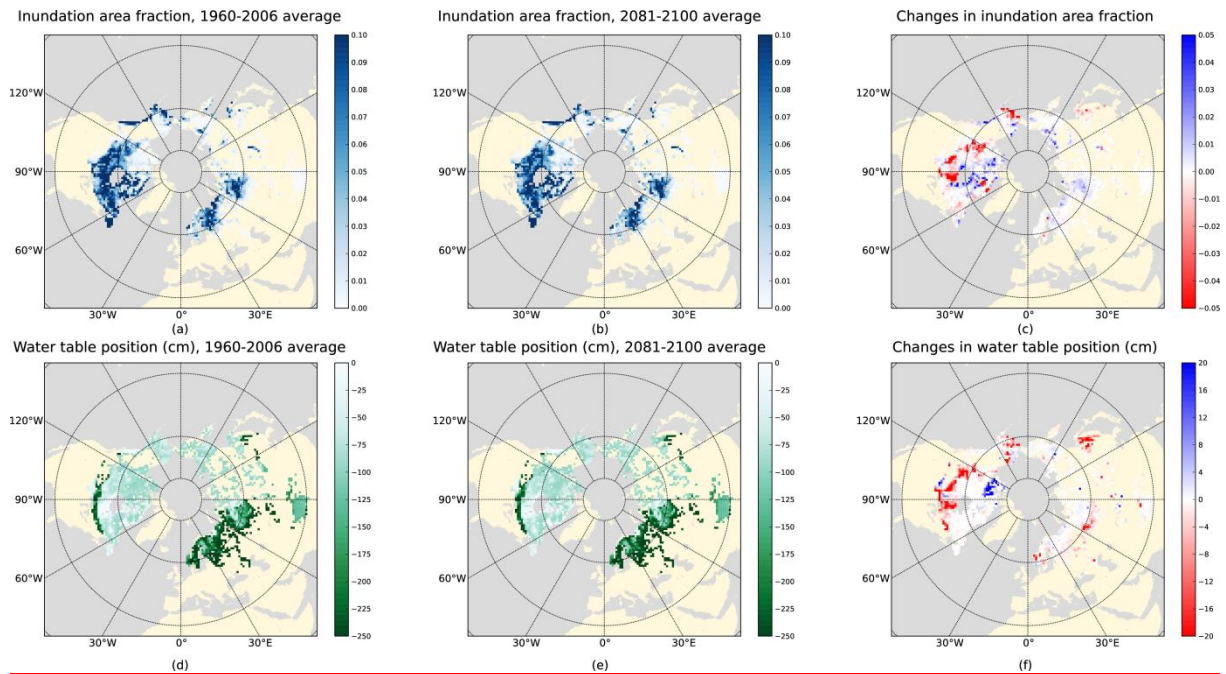

(a) Inundation area fraction, 1960-2006 average
(b) Inundation area fraction, 2081-2100 average
(c) Changes in inundation area fraction
(d) Water table position (cm), 1960-2006 average
(e) Water table position (cm), 2081-2100 average
(f) Changes in water table position (cm)

Figure 13. Changes in inundat~~ioned~~ ~~condition~~area fraction and ~~ground~~ water table ~~level~~position during the historical period (1960-2006) and projection period (2081-2100). ~~The projected results were calculated based on the full simulation~~ for the process-based projection. Panel (a) is the average inundation fraction during 1~~2~~960-2006, (b) is the average of 2081-2100; (c) is the difference between these 2 averages (panel b - a). Panels (d)-(f) are similar for ~~ground~~ water table ~~levels~~positions.